SMC-TR-02-24

AEROSPACE REPORT NO.
TR-99(1413)-6

Viton® B O-Ring Resilience Study

26 January 2001

Prepared by

T. W. GIANTS
Space Materials Laboratory
Laboratory Operations

Prepared for

SPACE AND MISSILE SYSTEMS CENTER
AIR FORCE MATERIEL COMMAND
2430 E. El Segundo Boulevard
Los Angeles Air Force Base, CA 90245

Space Systems Group

THE AEROSPACE CORPORATION
El Segundo, California

This report was submitted by The Aerospace Corporation, El Segundo, CA 90245-4691, under Contract No. F04701-00-C-0009 with the Space and Missile Systems Center, 2430 E. El Segundo Blvd., Los Angeles Air Force Base, CA 90245. It was reviewed and approved for The Aerospace Corporation by P. D. Fleischauer, Principal Director, Space Materials Laboratory. LTC D. Lileikis was the Titan Chief Engineer.

This report has been reviewed by the Public Affairs Office (PAS) and is releasable to the National Technical Information Service (NTIS). At NTIS, it will be available to the general public, including foreign nationals.

This technical report has been reviewed and is approved for publication. Publication of this report does not constitute Air Force approval of the report's findings or conclusions. It is published only for the exchange and stimulation of ideas.

LTC D. Lileikis, USAF
SMC/CLT

REPORT DOCUMENTATION PAGE

Form Approved
OMB No. 0704-0188

1. AGENCY USE ONLY (*Leave blank*)	2. REPORT DATE	3. REPORT TYPE AND DATES COVERED
	26 January 2001	

4. TITLE AND SUBTITLE

Viton® B O-Ring Resilience Study

5. FUNDING NUMBERS

F04701-00-C-0009

6. AUTHOR(S)

T. W. Giants

7. PERFORMING ORGANIZATION NAME(S) AND ADDRESS(ES)

The Aerospace Corporation
Technology Operations
El Segundo, CA 90245-4691

8. PERFORMING ORGANIZATION REPORT NUMBER

TR-99(1413)-6

9. SPONSORING/MONITORING AGENCY NAME(S) AND ADDRESS(ES)

Space and Missile Systems Center
Air Force Materiel Command
2430 E. El Segundo Boulevard
Los Angeles Air Force Base, CA 90245

10. SPONSORING/MONITORING AGENCY REPORT NUMBER

SMC-TR-02-24

11. SUPPLEMENTARY NOTES

12a. DISTRIBUTION/AVAILABILITY STATEMENT

Approved for public release; distribution unlimited

12b. DISTRIBUTION CODE

13. ABSTRACT (*Maximum 200 words*)

The Challenger accident in January 1986 was attributed to failure of the pressure seal in the aft field joint of the solid rocket motor. It was concluded that the elastomeric O-ring seals did not perform their sealing function because of the low temperatures at launch. Because the Shuttle and Titan O-rings were both made of Viton, there was concern that the O-rings on the segment tang and clevis joints on the Titan solid rocket motor might cause a similar problem. Launch delays that exceeded the assembled segment O-ring service life of 12 months also raised concerns. These delays resulted in the initiation of a pad-life extension program and a reevaluation of the O-ring seal. Structural analysis of clevis joint motion had predicted that a gap could be generated at the clevis joint where the O-ring is seated. This gap must be closed by O-ring decompression to maintain the seal during ignition, pressurization, and flight. This decompression (determined by the resilience of the O-ring) must take place rapidly enough to seal the clevis joint in advance of increasing exhaust gas pressure.

This report presents data on the resilience characteristics of Viton B ® O-rings under long-term compression in real time. These data can be used in conjunction with structural analysis of joint motion to predict joint seal performance during installed seal lifetime. The resilience of Viton ® B O-rings was measured as a function of initial 17% and 23% compression, time under compression up to 3 years, test temperatures of 60°F and 70°F, and O-ring lot. The results showed that resilience of Viton B O-rings is reduced significantly as the temperature is lowered and with increasing time under compression, which is of concern when segments are stacked for long periods of time. The results also indicate that, in the absence of side-pressure assist, a no leak condition exists only for the shortest times under compression and particularly at the higher temperature condition. Since successful Titan launches have occurred with pad life as long as 14 months, it appears that side pressure-assisted recovery is essential to O-ring sealing ability.

14. SUBJECT TERMS	15. NUMBER OF PAGES
Fluorinated elastomer, Compression set, Aging, Solid rocket motor, joint seal	52
	16. PRICE CODE

17. SECURITY CLASSIFICATION OF REPORT	18. SECURITY CLASSIFICATION OF THIS PAGE	19. SECURITY CLASSIFICATION OF ABSTRACT	20. LIMITATION OF ABSTRACT
UNCLASSIFIED	UNCLASSIFIED	UNCLASSIFIED	

Acknowledgments

The author wishes to thank R. M. Castaneda and R. A. Shenk for their diligence and attention to detail in sample test assembly and measurement techniques, and P. D. Chaffee for writing the software program for data conversion. The author also wishes to thank Dr. S. L. Zacharius for initiating this project and for her many technical contributions during the course of this work, and Dr. R. A. Lipeles for technical discussions in the preparation of this report.

The author also wishes to thank M. Buechler of the Titan Program Office for support of this effort and for providing important details regarding the SRM structure and environment.

Contents

Figures

Tables

1. Introduction

The Presidential Commission on the Shuttle Challenger accident on mission 51-L in January 1986 concluded that the cause was the failure of the pressure seal in the aft field joint of the solid rocket motor. The Commission also stated that the elastomeric seals were severely affected (hardened) by the low temperatures at launch.[1] The Challenger accident raised a number of issues that led to a redesign of the Shuttle field joint.[2–4] As a result of the accident, the Air Force became concerned that the O-rings on the segment tang and clevis joints of the Titan solid rocket motor (SRM) might cause a similar problem. Although processed differently, the Shuttle and Titan O-rings were both made of Viton®, a fluorocarbon elastomer. The Shuttle program used an extruded material, which was spliced in 3–5 places, while the Titan solid rocket motor (SRM) program used a single, molded Viton O-ring.

Among the original design requirements for the Titan SRM O-ring seal was a minimum 17% compression squeeze, operating temperatures from 40° to 90°F, and a 12-month assembled life. Subsequent to the Challenger accident, joint heaters were evaluated by Titan and then applied to SRM joints so that O-ring temperatures were maintained above 60°F. During the Titan SRM program, a number of circumstances led to launch delays where the assembled segment design lifetime of 12 months was exceeded. These delays resulted in the initiation of a pad-life extension program and subsequent reevaluation of the O-ring seal. Taken together, the concern of the impact of these conditions on long-term O-ring integrity was the impetus for this effort on Viton B material properties.

The Titan IV SRM consisted of seven D6AC high-strength steel alloy case segments and two closures that were mechanically fastened using clevis-tang joints. Each of the eight field joints utilizes a single continuously molded O-ring. The clevis-tang O-ring joint was designed to accommodate the structural deflections arising during ignition, lift-off, and flight. The O-rings must be resilient enough to respond rapidly to the maximum expected gap opening due to joint motions resulting from these structural deflections.[5] A cross section of the SRM field joint design, including additional insulation features, is shown in Figure 1.

Viton B was the material used in the O-rings that sealed the Titan SRM clevis joints. Viton B is a fluorocarbon terpolymer manufactured by the Du Pont Company and is prepared from vinylidene fluoride, hexafluoropropylene, and tetrafluoroethylene monomers. The monomer ratios employed, combined with a specific catalytic curing system, are designed to confer elastomeric properties for a wide variety of sealing applications.[6–8] The O-ring material performed its critical sealing function during the launch phase and duration of the solid rocket booster phase.

The initial igniter flame front ignites the segments' propellant surfaces, resulting in a rapid pressure build-up to the maximum expected operating pressure (MEOP). During this time, the steel membranes of the case barrel outward to produce a rolling motion to the joint, which, in turn, pushes the tang and outer clevis leg apart. The pressurized gas (side pressure) penetrates the putty and, through multiple charging paths, pressurizes the joint area, further opening the gap and also pushing the O-ring into place. Deformation resulting from internal pressurization of the case is commonly referred

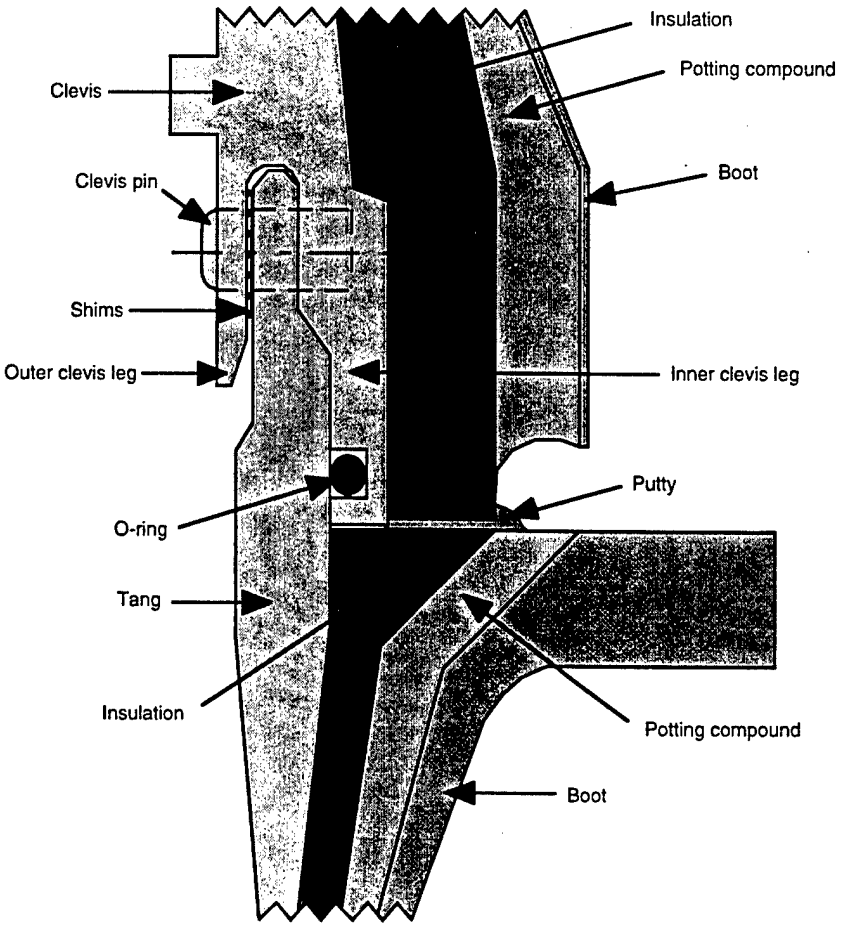

Figure 1. Cross section of Titan IV SRM field joint assembly.

to as joint roll. An illustration of the gap that is generated by this joint motion is shown in a schematic of the clevis joint in Figure 2. Any gap that develops must be closed by O-ring expansion to maintain the seal during booster lifetime. The resilience or recovery properties of the O-ring must provide this gap-sealing capability.[9] This O-ring expansion must take place rapidly enough to seal the clevis joint in the initial 0.5 s, the point at which the vehicle's MEOP is reached.

The gap displacement at the clevis joint during the launch phase that is predicted by structural analysis is shown in Figure 3. Curve A in Figure 3 represents the predicted gap opening history for simultaneous initial pressurization of both the case and joint area, reaching a maximum gap displacement of 0.034 in. Curve B represents the predicted gap opening history for case pressurization and an unpressurized O-ring, reaching a maximium gap displacement of 0.019 in. During the period until MEOP is reached, the O-ring must accommodate the gap opening and withstand the side pressure from ignition, thereby sealing the joint. During delayed pressurization of the joint area, where joint roll precedes O-ring pressurization, the gap opening initially follows curve B. As the O-ring is pressurized, the gap opening rapidly transitions to follow curve A, and an equilibrium pressure condition is attained between the joint and the vehicle's MEOP. Failure to maintain this equilibrium

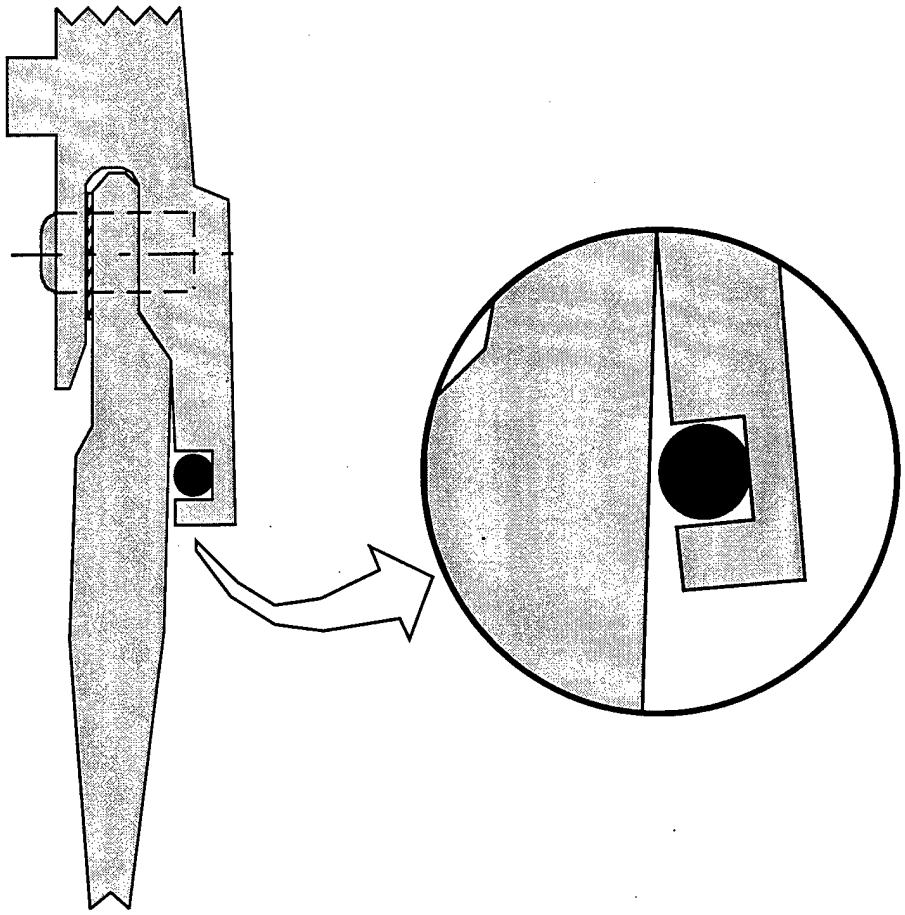

Figure 2. Cross section of field joint and enlarged area of O-ring region exhibiting deformation at the joint.

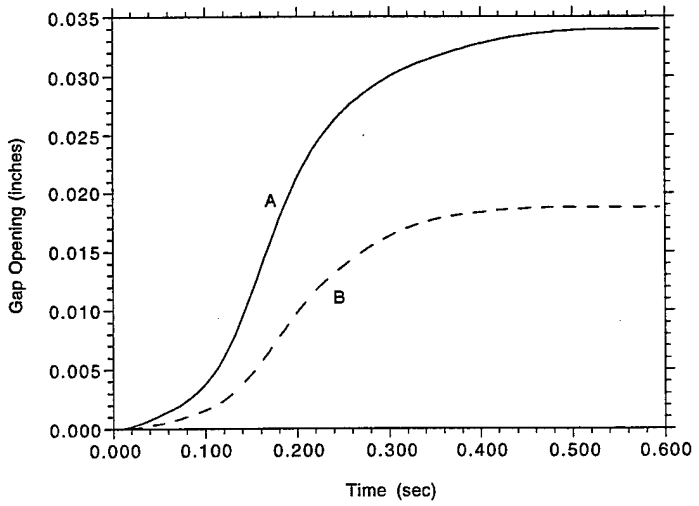

Figure 3. Predicted Titan SRM O-ring gap opening with time. (A) Displacement history for O-ring pressurized at ignition. (B) Displacement history for unpressurized O-ring.

sealing condition could result in potential joint failure due to the flow of unimpeded exhaust gases at high temperature.

The performance of the O-ring is critical to joint seal integrity. Seal performance depends both on the deflection and the deflection rate. The resilience of an elastomer is defined as "the ratio of energy output to energy input in a rapid or instantaneous full recovery of a test piece."[10] (Resilience here describes the capability of the O-ring material to respond to joint motion.)

With delays in programs resulting in storage situations exceeding the specified service life of the Viton B O-ring seals under the field joint environment, a reassessment of joint seal issues was undertaken. The focus of this assessment was the effect of long-term aging on the resilience of the O-ring material and also the effect of temperature on this property.[11]

The purpose of this report is to present some long-term resilience data for O-rings made from Viton B. These data may be used in conjunction with structural analysis in order to improve performance predictability. The O-ring materials were evaluated at two different compression values and two temperatures for periods of up to three years. The O-ring used in the Titan clevis joint has a 115.4-in. inner diameter and a 0.275-in. cross section. Since it was impractical to simulate recovery tests of the actual O-ring because of its size, an experimental procedure was devised to test samples on a much smaller scale for extended periods.

There were a number of differences between the test fixture used to test the O-ring materials used in this study and the launch vehicle environment. A full-scale simulation would use an entire O-ring, eliminating the unconstrained open-face edge effects present in the linear sample configuration. With an aspect ratio of only 4:1 in the linear sample configuration, the effect of compression on resilience may deviate from that of the O-ring configuration. Because the ends of the samples are unconstrained, O-ring resilience values in the direction of decompression may not be fully realized. Although the linear sample configuration may result in lower values, the differences are not expected to be significant at this aspect ratio.

The O-ring samples are also bonded to a metal tab for attachment to the LVDT core. This attachment is confined to a small surface area of the O-ring, and its impact on resilience is also not considered significant.

The variability in the samples that make up the average for any time period can also be the result of inhomogeneities in the O-ring, which is not unusual for a filled system and the small sample size used. Because the viscoelastic properties of a whole O-ring should average out such inhomogeneities under decompression, the average of the individual sample values should be more representative than any one specific value.

2. Experimental

Since one of the goals of the work was to provide some useful trends in resilience when O-rings are subjected to launch delays, a number of samples were subjected to compression for periods of up to three years. A number of one-inch samples were cut from a manufactured O-ring made from Viton B that was qualified to be used as a Titan clevis joint seal. Each sample was subjected to one of two levels of compression (17% and 23% squeeze), the minimum and maximum values allowed within the Titan specification, and comparable with data obtained from a previous NASA study of O-rings. The sample holder consisted of a 2-in. by 2-in. by 1-in. thick aluminum block. A channel was machined that approximated the size of the O-ring groove of the clevis joint. A flat aluminum cover piece was machined to provide the mating surface. For measurement purposes, a metal strip slightly longer than the length of the sample and 0.008 in. thick to maintain planarity, was bonded to the Viton B sample using a thin layer of epoxy adhesive. A small hole was placed in one end of the metallic strip to provide an attachment location for the linear variable differential transformer (LVDT). The total thickness of the sample, including the adhesive and metallic strip, was measured, and the sample was placed in the groove with the metallic strip facing upward. A series of metal shims 0.001 in. thick are used in combination with the measured depth of the sample holder channel to approximate either the 17% or 23% compression squeeze. The shims are placed between the aluminum block and its cover piece, and the segments are bolted together. An illustration of the sample configuration and the parts used to construct the sample holder is shown in Figure 4.

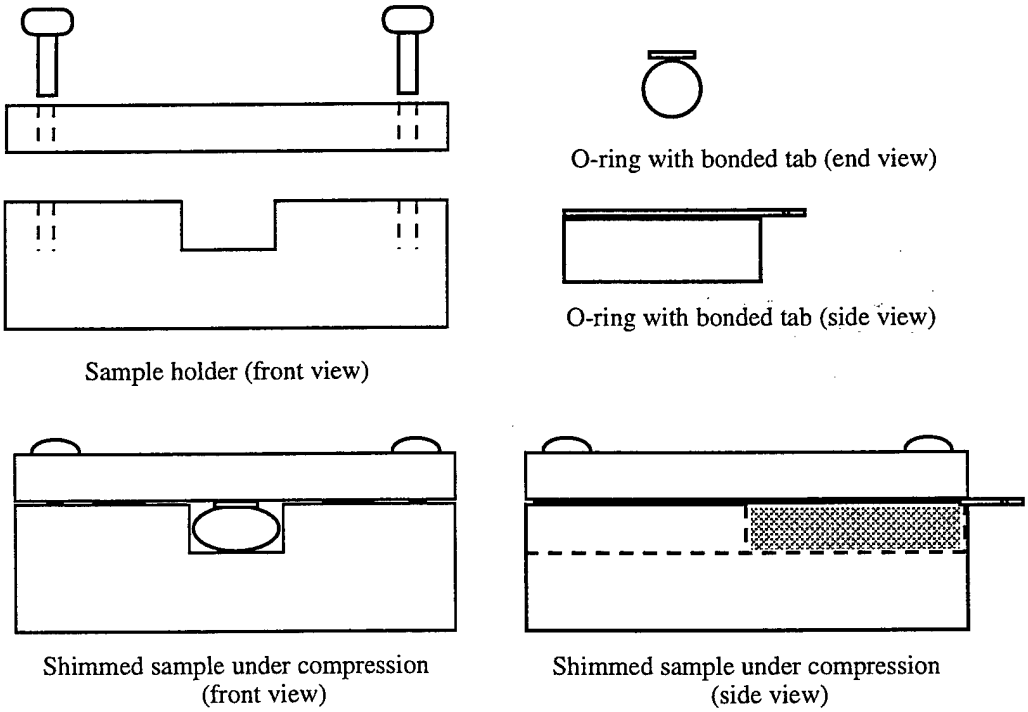

Figure 4. Example of O-ring configuration and sample holder construction.

The samples, configured as shown in Figure 4, were stored under ambient conditions for specific time periods. At the end of a selected time period the samples were tested at either ambient laboratory conditions, nominally 70°F, or at 60°F. The lower temperature test is performed by first cooling the sample to approximately 40°F in a refrigerator, placing the sample in the test fixture, and monitoring the sample temperature with a thermocouple. The experiment is initiated when the thermocouple records 60°F, typically about 10 min after removal from the refrigerator. Thermocouples are not used for the tests at ambient temperature. The test fixture itself, shown schematically in Figure 5, is fabricated from aluminum sheet stock .

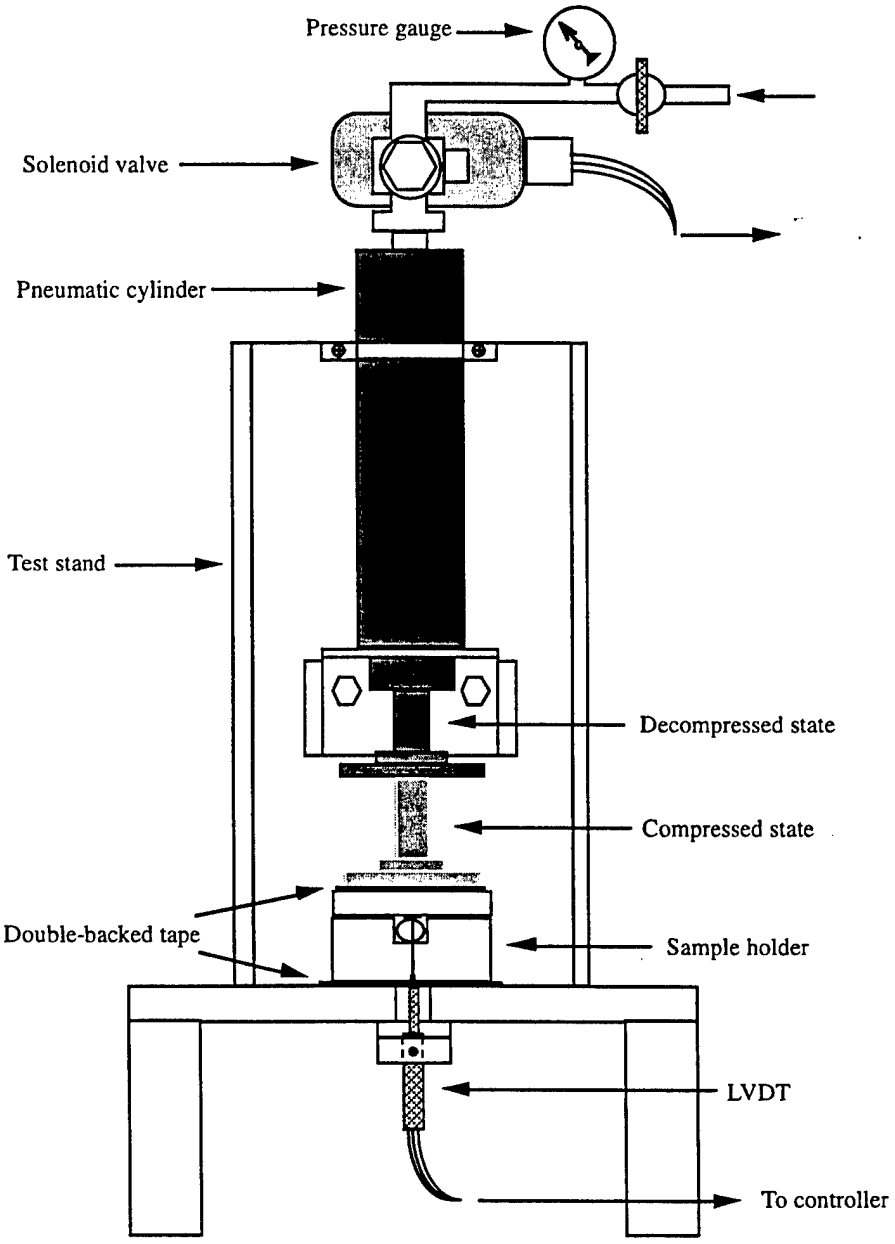

Figure 5. Illustration of test stand configuration with sample connected to LVDT assembly.

The O-ring sample was placed in the sample holder assembly so that the protruding end of the metallic strip overhung the holder, and the O-ring itself was kept flush with the edge of the holder. This positioning is depicted in the side view of the compressed shimmed sample in Figure 4. A linear variable differential transformer (LVDT) core is bonded to the metallic strip at the guide hole with epoxy adhesive as shown in Figure 5 (front view) and Figure 6 (side view).

Double-backed tape was used both to constrain the sample holder assembly to the test stand platform and to enable proper centering of the LVDT core into the LVDT coil as indicated by a zero voltage reading on a digital multimeter. Double-backed tape was also placed on the contact plate of the cylinder rod. The pneumatic cylinder was then pressurized to 30 psi, and the screws holding the upper plate of the sample holder were removed. This procedure retained the original compression on the

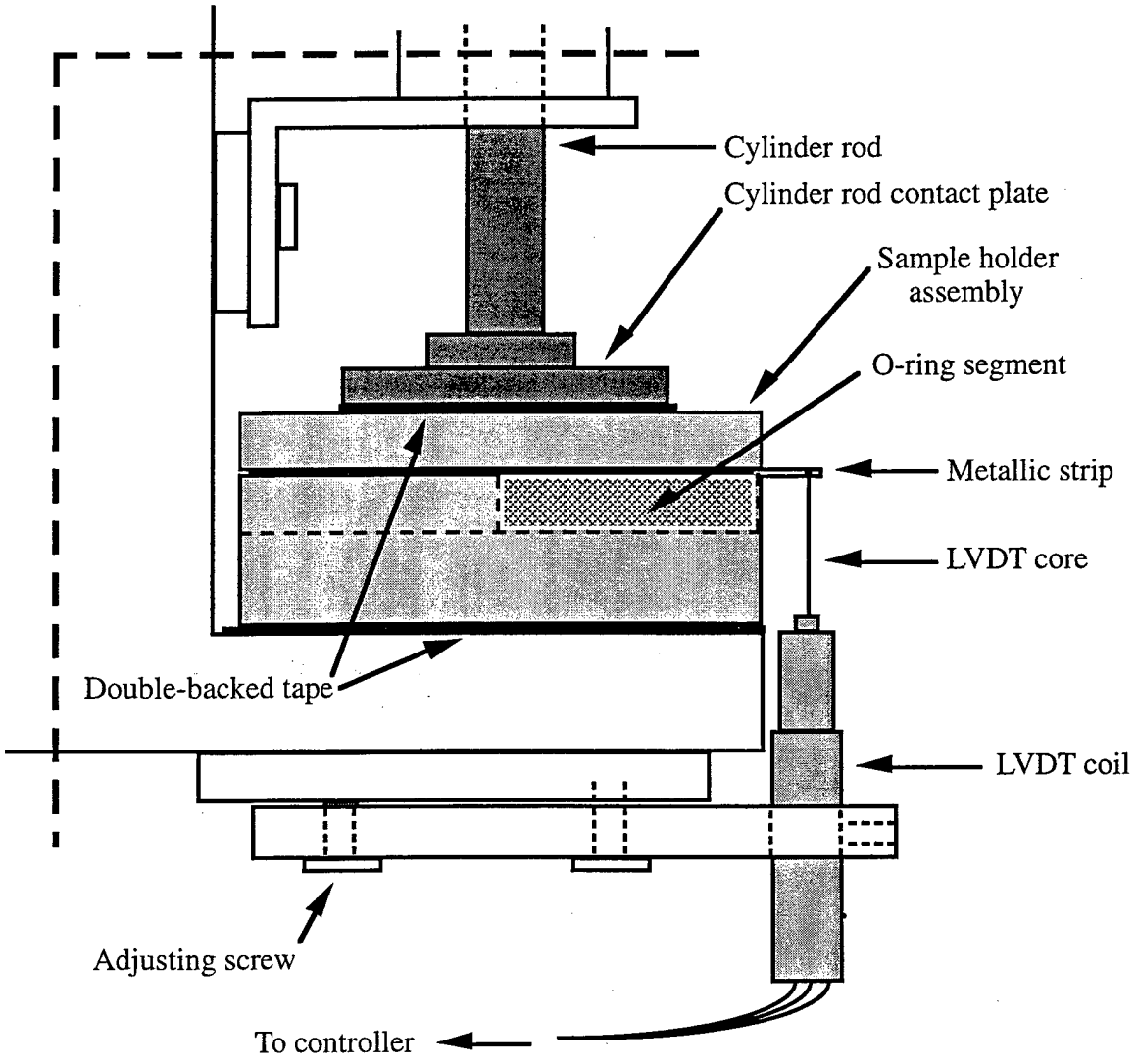

Figure 6. Cutaway section of test stand assembly illustrating sample to LVDT connection.

sample while firmly attaching the sample cover plate to the contact plate of the cylinder rod. The LVDT, which produces an electrical output proportional to the displacement of its separate movable core, was then re-zeroed by means of the adjusting screw indicated in Figure 6. The LVDT assembly was initially calibrated to produce a curve of voltage vs displacement measured in inches. When decompression was initiated, the cover plate of the sample holder was removed from interference with the LVDT measurement while the bottom plate was secured from undesirable movement. Prior to collecting data it was established that removal of the sample cover plate was faster than the rebound of the O-ring. Thus, the sample cover plate did not affect the resilience measurements.

After the components were assembled as described above, a test was performed by initiating a computer program that first includes a pre-trigger delay of 100 ms, which activates both a computer and recorder. At time zero (0.100 s elapsed time), the solenoid valve was triggered causing decompression of the pneumatic cylinder and removing the constraining force on the O-ring assembly. Since the displacement of the LVDT core was coincident with the decompression of the O-ring, the dimensional change in the O-ring was transmitted as a change in voltage. The voltage data were collected at the rate of 500 data points per second during a 2-s test period and stored. The voltage data were converted to units of a linear dimension (inches), and changes were recorded vs elapsed time. A test matrix using available Viton B fluoroelastomer O-ring samples is shown in Table 1.

The three Viton B samples used in the test matrix shown in Table I consisted of two O-rings of identified origin, S/N 2203 and S/N 3060, and one with an unknown pedigree (UNK). All three batches were qualified Titan flight hardware. Tests performed under 17% compression used S/N 2203, and tests performed under 23% compression used S/N 3060 in order to preserve batch integrity. With the remaining O-ring material, batch-to-batch variability was compared for the three O-rings at one temperature, 70°F, for three time intervals, 1 week, 12 months, and 24 months. This matrix was necessary due to the lack of availability of any one material lot to accommodate the entire set of conditions.

Table 1. Compression/Temperature Test Matrix for O-ring Samples S/N 2203, S/N 3060, and UNK.

Batch Conditions	S/N 2203 (17%)		S/N 2203 (23%)	S/N 3060 (17%)	S/N 3060 (23%)		UNK (17%)	UNK (23%)
Period	60°F	70°F	70°F	70°F	60°F	70°F	70°F	70°F
24 h	x	x	-	-	x	x	-	-
1 wk	x	x	x	x	x	x	x	x
2 wk	x	x	-	-	x	x	-	-
1 mo	x	x	-	-	x	x	-	-
2 mo	x	x	-	-	x	x	-	-
3 mo	x	x	-	-	x	x	-	-
6 mo	x	x	-	-	x	x	-	-
12 mo	x	x	x	x	x	x	x	x
18 mo	x	x	-	-	x	x	-	-
24 mo	x	x	x	-	x	x	x	-
30 mo	-	x	-	-	-	x	-	-
36 mo	x	x	-	-	x	x	-	-

The Viton B fluorocarbon samples were cut from the large O-rings described above, with each sample set consisting of five 1-in. pieces cut consecutively. The average of the five samples used for a specific set of conditions was used to represent the recovery capability of the material under those conditions. A number of factors may come into play that do not fully represent the absolute response of a complete O-ring. Among these are: (1) the exposed ends of the samples can deform without the mechanical resistance present in a complete O-ring; (2) variations in bulk properties throughout the length of a processed O-ring can lead to variations in any average of five samples; (3) variations in physical attachment of the metallic strip to the O-ring can produce surface area effects; and (4) the fixed shim size does not fully meet the dimensions required for the 17% or 23% compression. However, the trends that are produced for the material under study are nonetheless very important in understanding its behavior.

This report will first discuss the results obtained for the individual batches followed by a discussion of comparative data among batches. Unlike the conditions present in the Titan SRM system, this initial phase of the study was performed in the absence of any silicone grease used to lubricate the O-ring and the O-ring gland. Where material availability allowed, a second phase of the study compared resilience behavior both in the presence and in the absence of lubricant.

3. Results for S/N 2203 Under 17% Compression

The studies were performed for different time periods, first for a 24-h period, and then periodically up to and including a 36-month period. The data were taken for a duration of 2 s, the time allowed for the O-ring to provide sealing capability. A representative comparison of the recovery of S/N 2203 at both 70°F and 60°F is seen in Figure 7 for a sample compressed at 17% for a 24-h period.

As can be seen in Figure 7, after the initial 100-ms programmed delay period, the rate of recovery at both temperatures is quite rapid for the first 100 ms of the test prior to falling to a much reduced rate for the remainder of the 2-s test period. Notable, of course, is the difference in overall recovery of the samples measured at the two temperatures. Even though the difference in temperature is only 10°F, the sample measured at 60°F recovered only 37% from its compressed state compared to the sample measured at 70°F, which recovered to nearly 50%. Thus, for an operating temperature reduction of only 10°F, there is a recovery loss of nearly 25%. To assure effective recovery properties for sealing purposes, external heaters are used around the clevis joint area of launch vehicles using O-rings made from Viton B.

Viton B has excellent *compression set properties, described as the percent of deflection by which an elastomer fails to recover after a fixed time under specified squeeze and temperature.* However, its resilience, which is the ability to return quickly to its original shape after a temporary deflection, is compromised by the effect of temperature on its hardness. Such an effect can be seen in a comparison of a variety of elastomers shown in Figure 8.

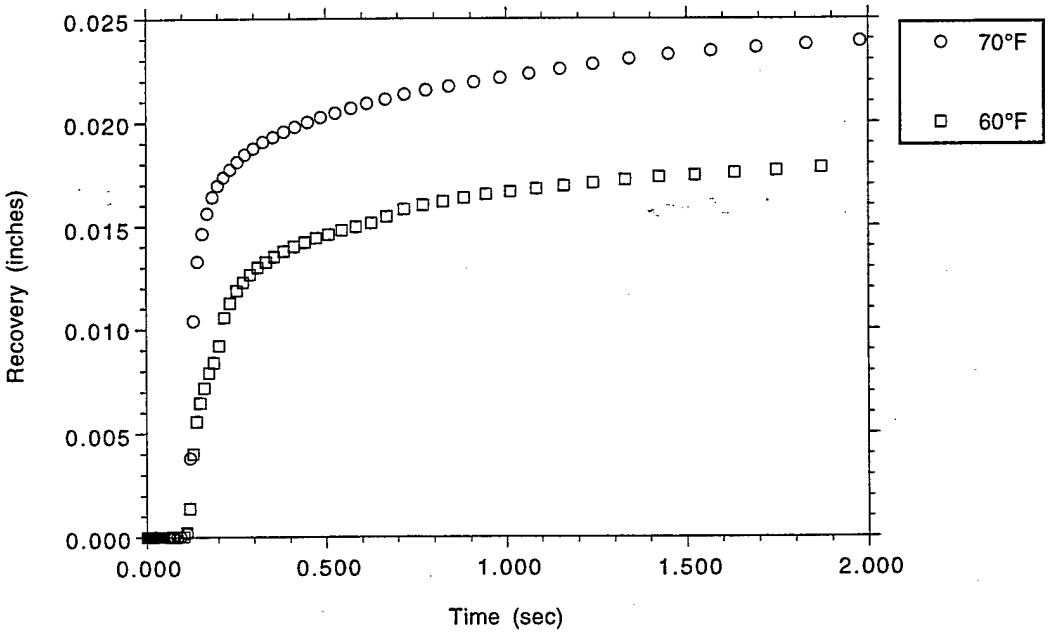

Figure 7. Recovery of Viton B S/N 2203 under 17% compression for a 24-h period.

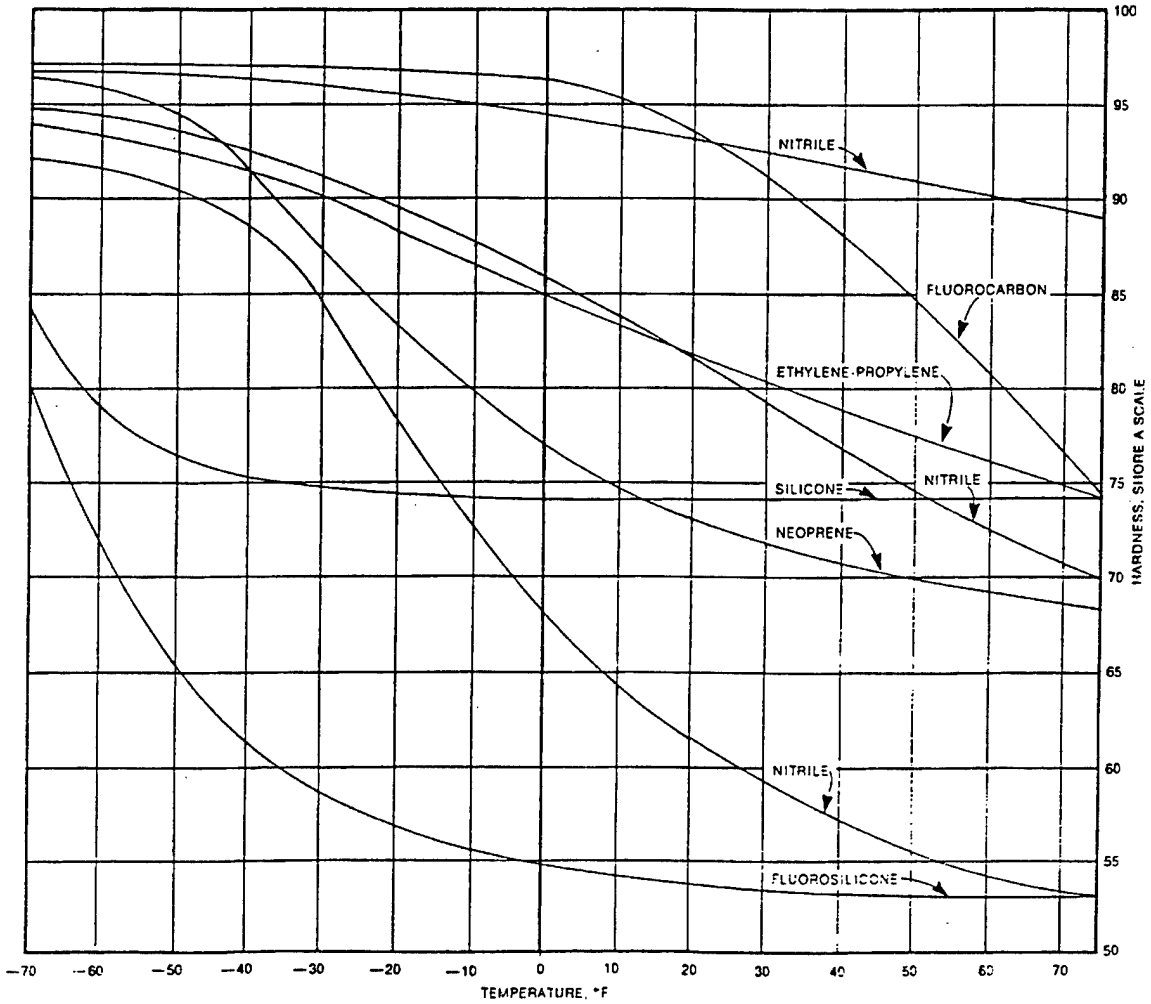

Figure 8. Effect of low temperature on rubber hardness (Parker O-Ring Handbook, 1992, p. A3-10; used by permission).

The fluorocarbon curve[12] shown in Figure 8, which is representative of the Viton B used in this study, shows a significant change in hardness value in the range of 60–70°F when compared to the other classes of elastomeric materials. It appears that this change in hardness translates to a much greater loss in resilience than would otherwise be expected for the very narrow temperature range chosen. This effect is further supported by data describing the dramatic decrease in resilience as the glass transition temperature (T_g) is approached.[13] For a Viton B material, the T_g is of the order of –4°F (–20°C), and the effect of temperature on resilience can be pronounced.[14]

Similarly, a comparison of the recovery of S/N 2203 at both 70°F and 60°F for a sample compressed at 17% for a 24-month period is seen in Figure 9. When compared with the results for the 24-h data in Figure 7, the results for the 24-month data in Figure 9 show recovery of less than half that in Figure 7. This is in agreement with the effects of long-term compression set on the viscoelastic behavior of this material.

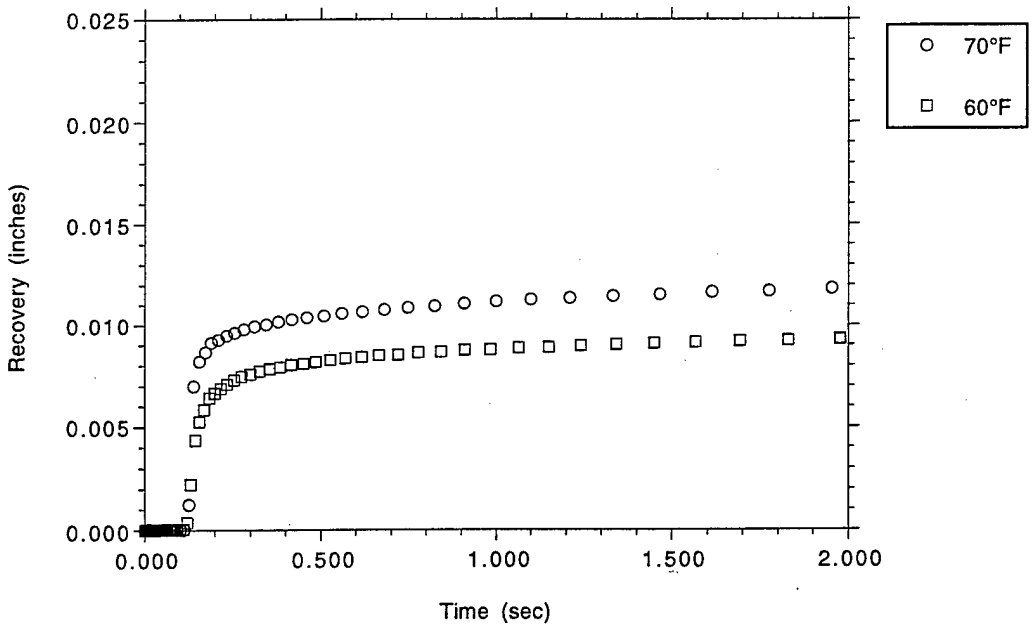

Figure 9. Recovery of Viton B S/N 2203 under 17% compression for a 24-month period.

Consistent with the difference in recovery observed for the samples in Figure 7, the recovery at 60°F is less than that at 70°F by approximately 22%. Again the rate of recovery is rapid during the first 100 to 200 ms before tapering off for the remainder of the test period.

For each time period where samples were compared, the samples measured at 60°F had a lower recovery rate than those measured at 70°F. Figures 10 and 11 show a composite of the recovery data for all the time periods measured for 17% compression at 70°F and 60°F, respectively. With longer time under compression the effect on resilience appears to level off as shown in the data after 18 months. The numbers in parentheses in the legend represent the number of samples used in the averages if less than the original five. The reduced numbers are the result of various equipment malfunctions in which case no data were obtained. Also seen during the initial delay period in these figures are some deviations from the zero point. Close inspection of the data indicates that these are due to random electronic noise and not to material response.

In Figure 10, the 70°F data show some overlapping values, but the trend, in general, is for the recovery to be less with increasing time under compression. With the exception of the outlier data obtained after 6 months under compression, the overall results are in the expected order within the variability of the samples that make up the average value. The results observed beyond 6 months show little variation, indicating that most of the compression set occurs early, and recovery values change only gradually after a certain point. The results are similar in Figure 11 for the 60°F data, with the 6-month data again being the exception along with the inverted results for the 24-h and 1-week values. Due to a number of potential factors contributing to variability in the data, no attempt is made to provide a consistent interpretation. The data from both Figures 10 and 11 do suggest, however, that there is little difference in recovery values as time under 17% compression exceeds 6 months.

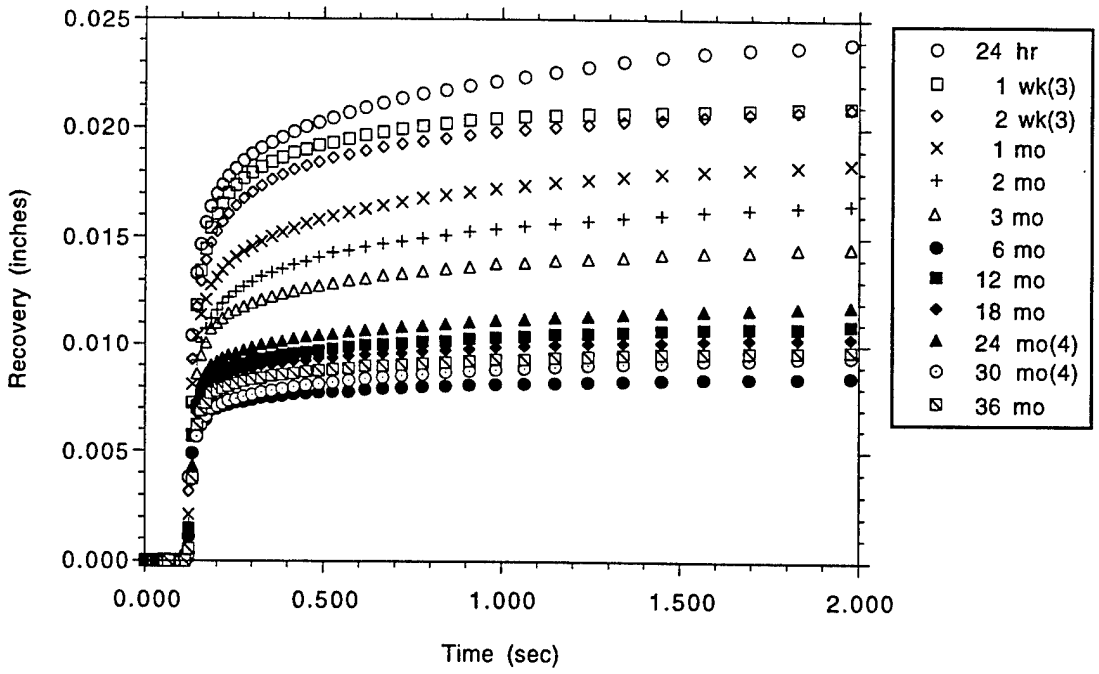

Figure 10. Recovery vs time for O-ring S/N 2203 under 17% compression measured at 70°F.

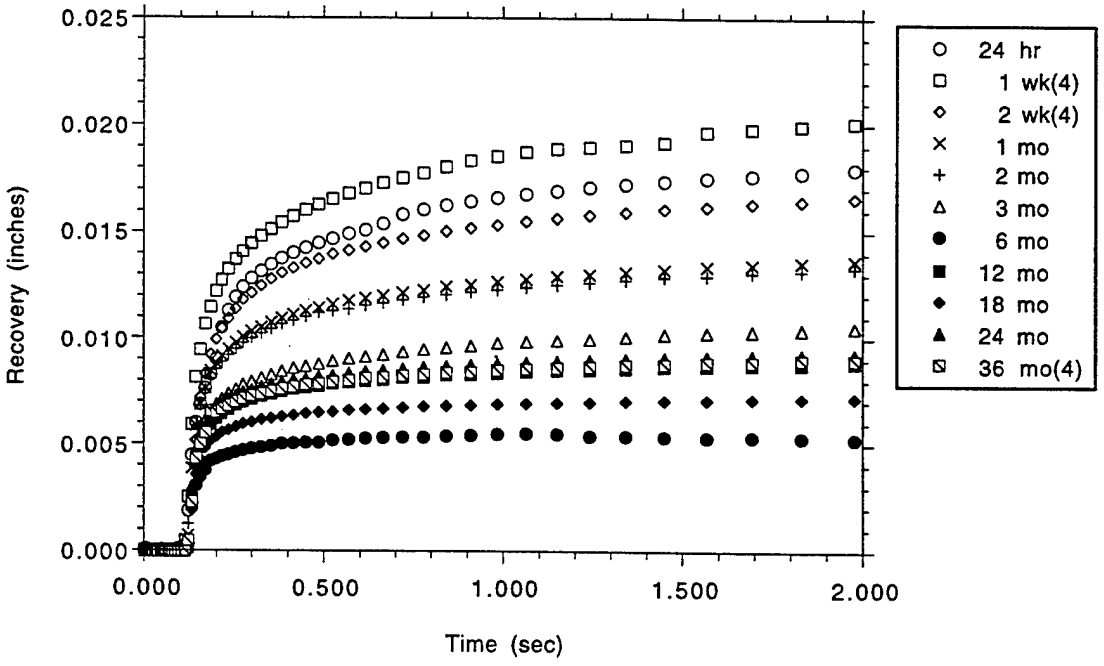

Figure 11. Recovery vs time for O-ring S/N 2203 under 17% compression measured at 60°F.

A more detailed look at the rate of recovery within the first 100 ms of the recovery period can be seen in Figure 12, where all the data points are shown for the 70°F samples. Deviation from smoothness in these curves is probably the result of uneven expansion of the samples following decompression. Electronic response times of the equipment used to trigger the decompression are on the order of 10 ms and are responsible for the lag in the recovery data seen in the first 20 ms.

The slopes of the curves in Figure 12 exhibit similar behavior with a rapid rate of change occurring through the first 135 ms. The initial rate of change then slows dramatically for all the samples, followed by a slow monotonic rise through the total test time of 2 s. Nearly 50% of the total recovery occurs during the first 135 ms, reaching approximately 75% after 200 ms. After this point, the relative difference in recovery value changes very little throughout the duration of the test. Although at first glance the behavior of the 6-month sample appears normal to about 130 ms, it appears significantly restrained beyond this point. At this time, there is no definitive explanation for this behavior.

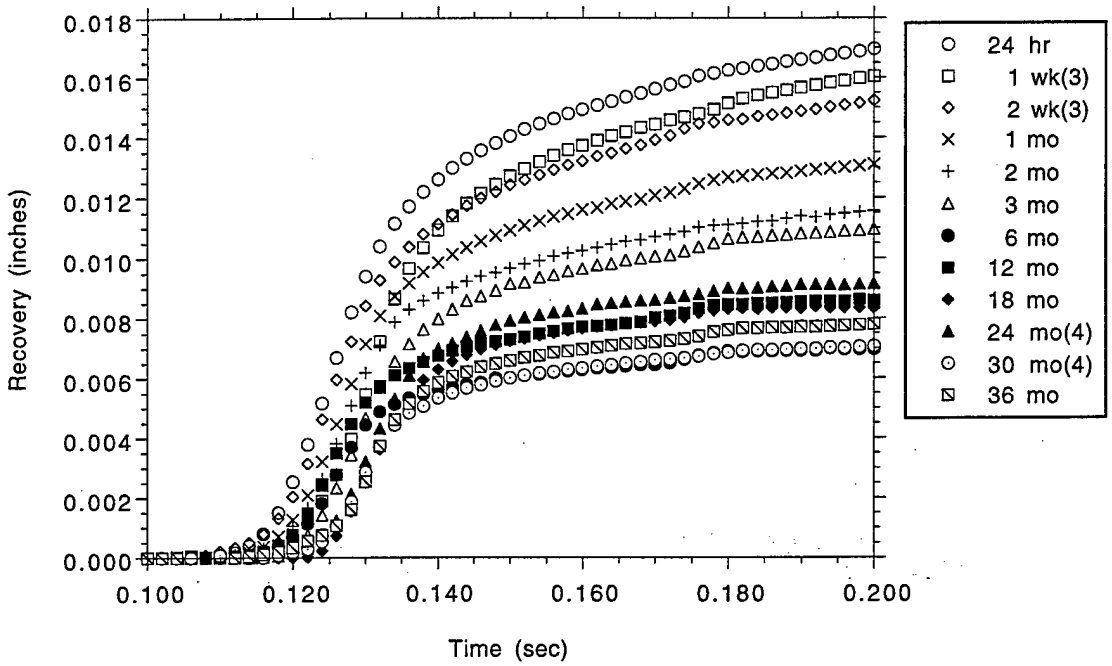

Figure 12. Recovery of S/N 2203 under 17% compression at 70°F during the initial 100-ms test period after the 0.1-s programmed delay.

4. Results for S/N 3060 Under 23% Compression

A separate O-ring designated S/N 3060 was used to study the behavior of Viton B under 23% compression. A comparison of the recovery of this O-ring for a 24-h period at both 70°F and 60°F is seen in Figure 13.

The results in Figure 13 are quite similar to the results for the 17% compression data shown in Figure 7, indicating less resilience at lower temperature. A rapid rate of change in the first 100 ms after the programmed delay is followed by a much lower rate of increase through the remainder of the 2-s test period. (However, as will be described later, comparative data for the same O-ring material under both 17% and 23% compression will show some variability. Compression set data for 17% and 23% compression for both O-ring batches, which are shown in Figure 20 later in this report, also illustrate this variability.) Thus, cross comparison of the data in this report should not be made until the batch-to-batch variability among O-ring materials is fully appreciated. Similarly, a comparison of the recovery of S/N 3060 at both 70°F and 60°F for a sample compressed at 23% for a 24-month period is seen in Figure 14. When compared with the results for the 24-h data in Figure 13, recovery for the 24-month period in Figure 14 is reduced by nearly half. Again, this is in agreement with the long-term compression set characteristics of the elastomer.

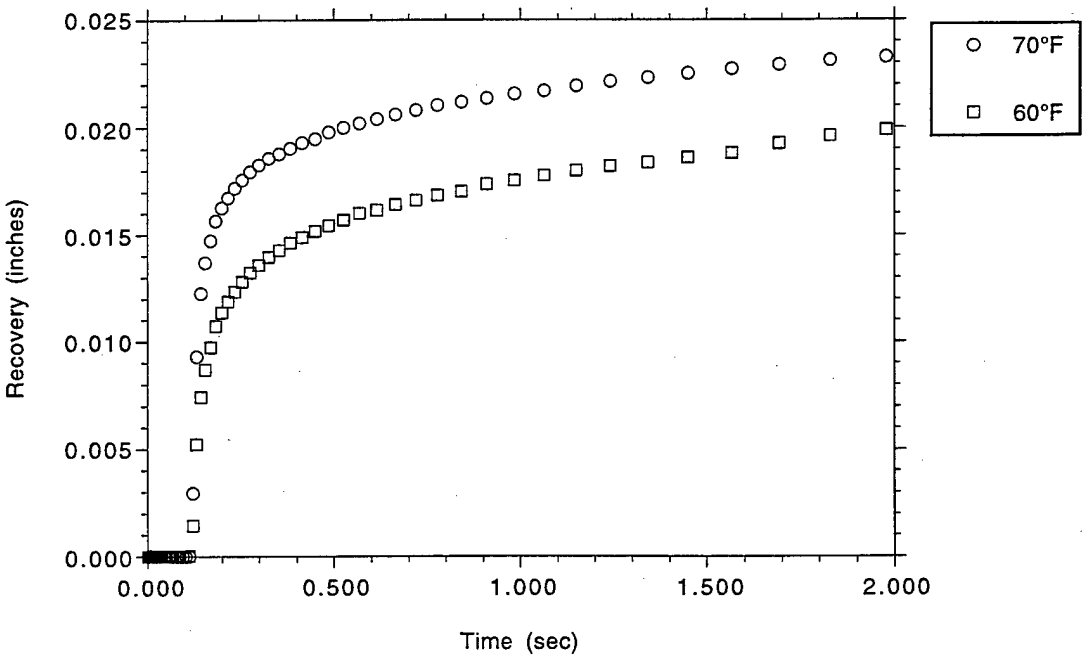

Figure 13. Recovery vs time for Viton B S/N 3060 under 23% compression for a 24-h period.

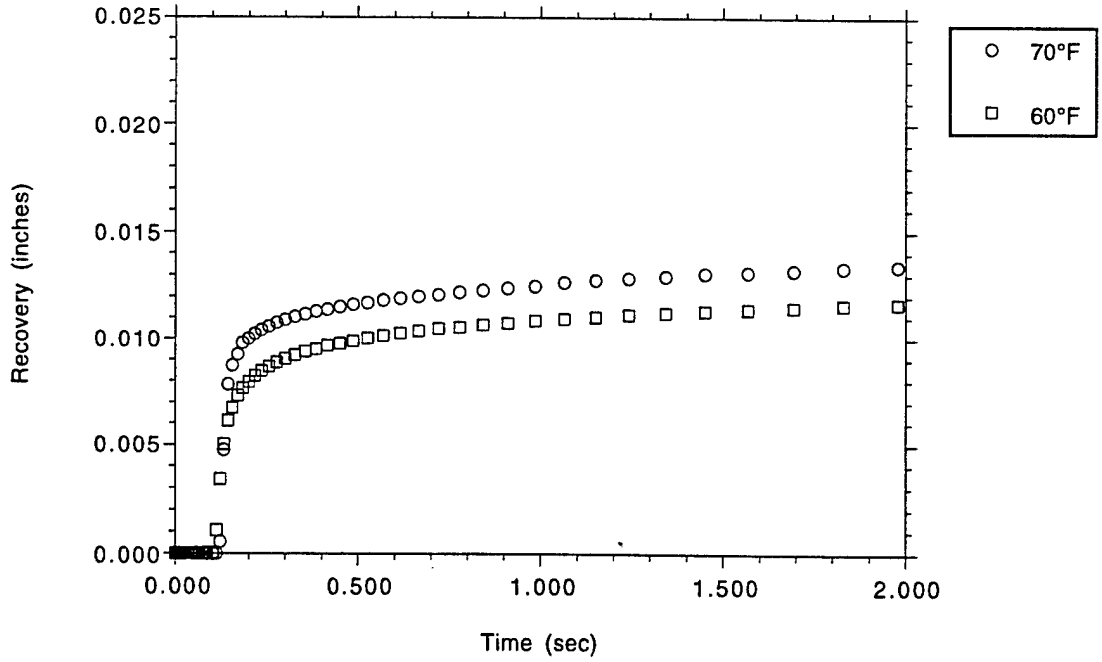

Figure 14. Recovery vs time for Viton B S/N 3060 under 23% compression for a 24-month period.

For each time period compared, the samples measured at 60°F had a lower recovery rate than those measured at 70°F. Again, with increasing time under compression, there appears to be a smaller effect on recovery rate with increasing time beyond the 3-month time period. Figures 15 and 16 show a composite of the recovery data for all the time periods measured for S/N 3060 at 70°F and 60°F, respectively. The results for O-ring S/N 3060 under 23% compression and 70°F indicate that the samples are more well behaved than those for the 17% compression data for S/N 2203, particularly with reference to the apparent anomalous data observed for the 6-month test periods. The trend of the data also shows the reduced ability of the O-ring material to recover as both time under compression is increased and temperature is lowered. However, the data for S/N 3060 for the 18-month period at 60°F also exhibits anomalous behavior in that it is positioned at nearly the same value as for the samples under compression for only a 1-month period. The results are seen in Figure 16.

Closer inspection of the data in Figure 16 reveals how the O-rings respond to decompression and, in some cases, where inconsistencies exist in the relative rates of recovery in the early stages vs those in the latter stages. This is seen more clearly in Figure 17.

Data for most of the time periods observed in Figure 17 appear to indicate similar behavior both in the early and latter stages of recovery. However, the recovery data for the 18-month period is quite erratic. Starting at a much lower rate than the others in the first 40 ms, it then appears to rise more quickly at the end of the first 100 ms (both indicated by the lower arrows in Figure 17). In so doing the total recovery of the 18-month sample becomes superimposed on that of the 1-month sample after the 2-s duration as seen in Figure 16. By contrast, the 24-month sample, although appearing to get an early start (upper arrow in Figure 17), has a rate of change throughout that is nearly identical to that of the 12-month sample. The behavior of the 18-month sample in Figure 16 is opposite to that of the 6-month samples in Figures 10 and 11. It is difficult to explain the 6-month data for S/N 2203 on the

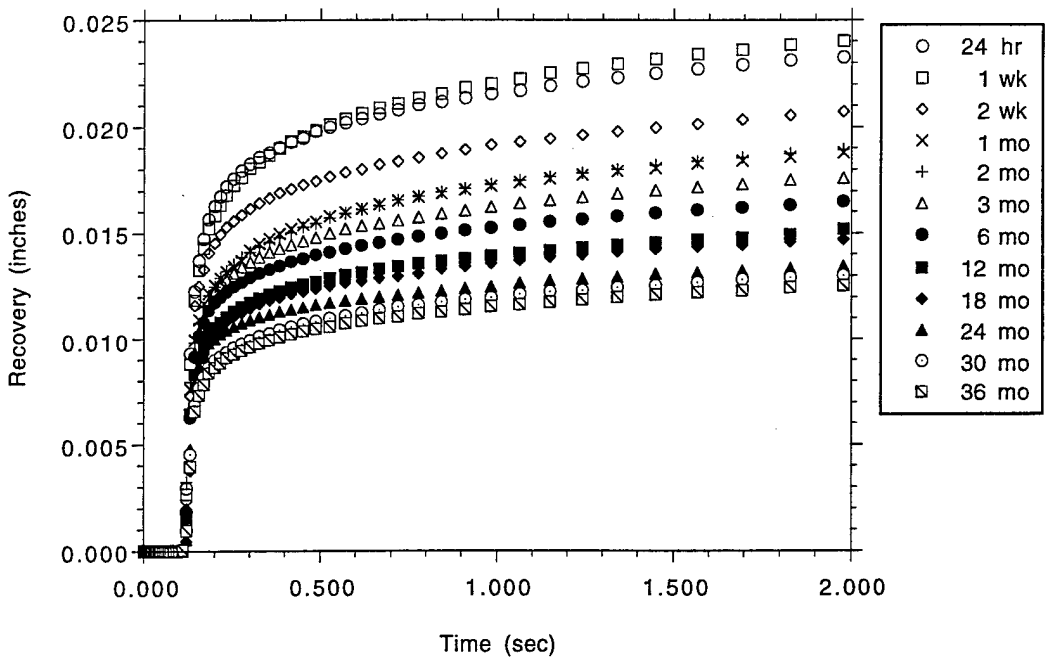

Figure 15. Recovery vs time for O-ring S/N 3060 under 23% compression measured at 70°F.

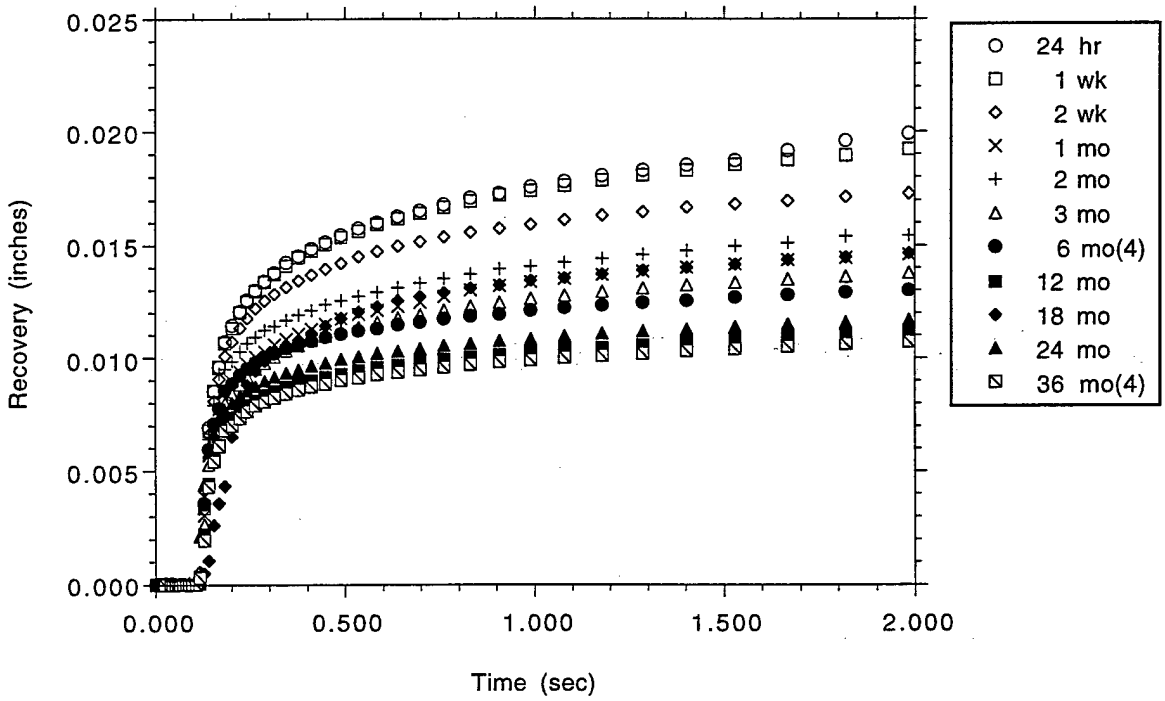

Figure 16. Recovery vs time for O-ring S/N 3060 under 23% compression measured at 60° F.

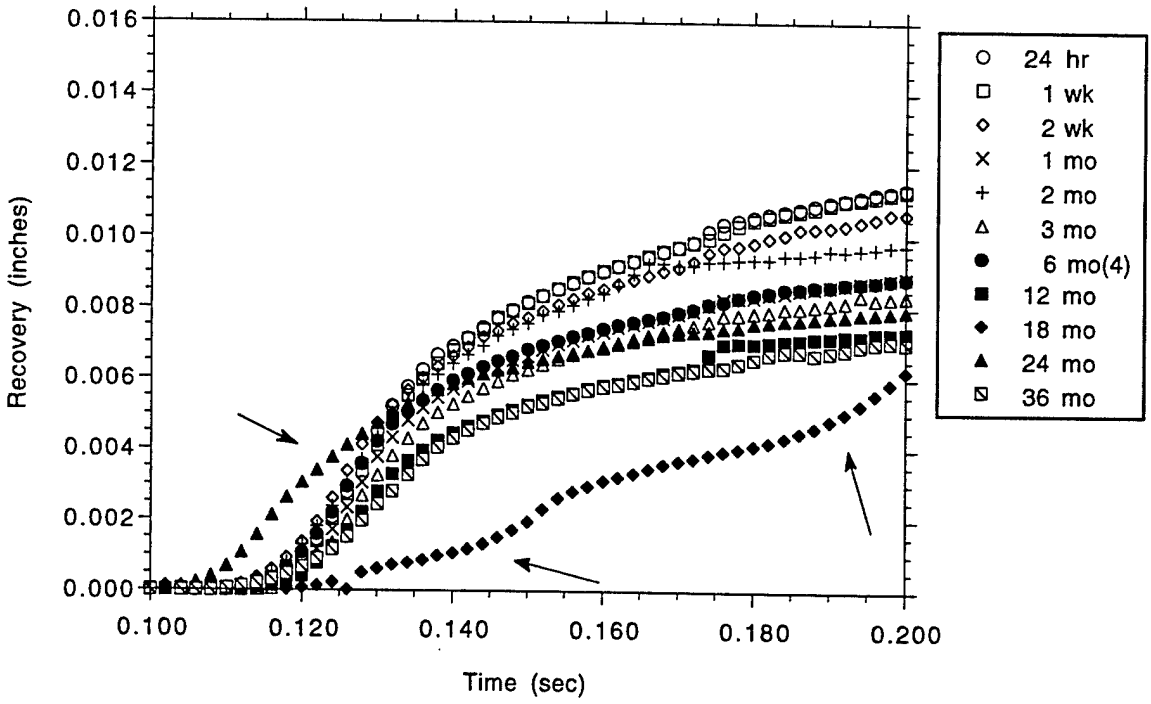

Figure 17. Recovery of S/N 3060 under 23% compression at 60°F during the initial 100-ms test period after the 0.1-s programmed delay.

basis of experimental error since both sample groups measured at 60°F and 70°F exhibit similar behavior. Also, any unusual transitions that may occur in the material during this time frame that might be responsible for the anomalous behavior are unsupported by the results for S/N 3060 at 6 months, where no comparable behavior is observed. One possibility is that inhomogeneities due to processing of the O-ring are responsible. This is likely to be the case in a filled elastomer. Since these data are made up from five samples cut sequentially from a segment, this is a likely assumption. One must be cognizant, however, that there is considerable variability within the data for each time frame, and that the absolute values are less significant than the relative values observed at different temperatures.

5. Results Under 17% and 23% Compression with Temperature

In order to appreciate the contribution of the individual samples to the averages used in assembling the recovery data for S/N 2203 in Figures 10 and 11 and the variability associated with those data, the averages are displayed in an alternate fashion as shown in Figure 18.

The results in Figure 18 incorporate the average of the 2.0-s data points taken for each of the test periods shown in Figures 10 and 11, and include the error limits from a calculation of the standard deviation. (It should be noted that the error limits shown at 2.0 s were at their maximum for each time period and essentially increased monotonically during the recovery period.) Inspection of the data shows significant variability, ranging from the lows for 70°F data at 12 months and 60°F data at 3 months to a high at 70°F and 2 months. Even allowing for the anomalous results reported for the 6-month periods, the trend of the data is fairly consistent with the overall expectation for a material under compression for an extended period.

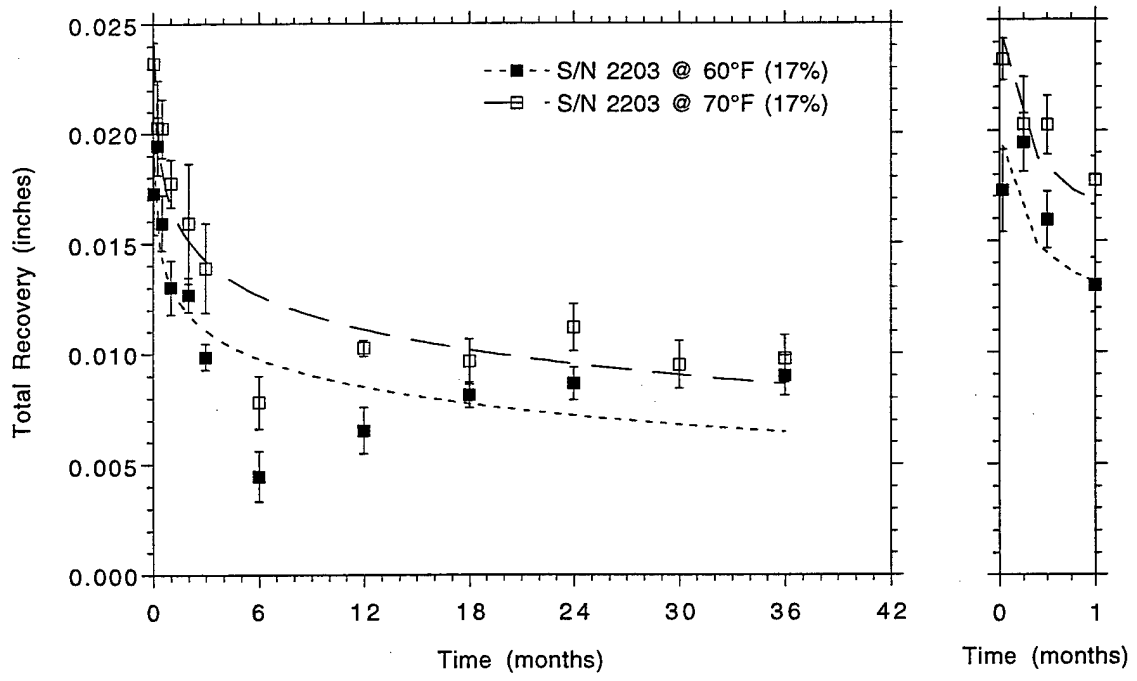

Figure 18. Comparison of total recovery at 2 s vs time under 17% compression for S/N 2203 measured at 60°F and 70°F. (Expanded 1-month recovery period is shown to the right.)

Similarly for the 23% data for S/N 3060, the variability within sample groups is also broad as shown in Figure 19. Again, with the exception of the anomalous data for 60°F at 18 months, which, coincidentally, is superimposed on the 70°F data, the trend is consistent with that seen for the 17% data for S/N 2203 in Figure 18.

In comparing the total recovery results for the samples under 17% and 23% compression in Figures 18 and 19, respectively, it is shown that recovery at the lower temperature (60°F) is consistently less than that at higher temperature (70°F). If one ignores the results for the samples ascribed to exhibiting the anomalous behavior described previously, then the rate of change in recovery is reduced dramatically somewhere in the 3- to 6-month time periods. Given the results from the time periods beyond 6 months, it appears that most of the compression set has taken place, and the recovery values are fairly predictable for long periods. At longer times, as stress relaxation becomes more complete, the elastic properties dominate, and the recovery at both 17% and 23% approximates a similar fraction of the original deflection.

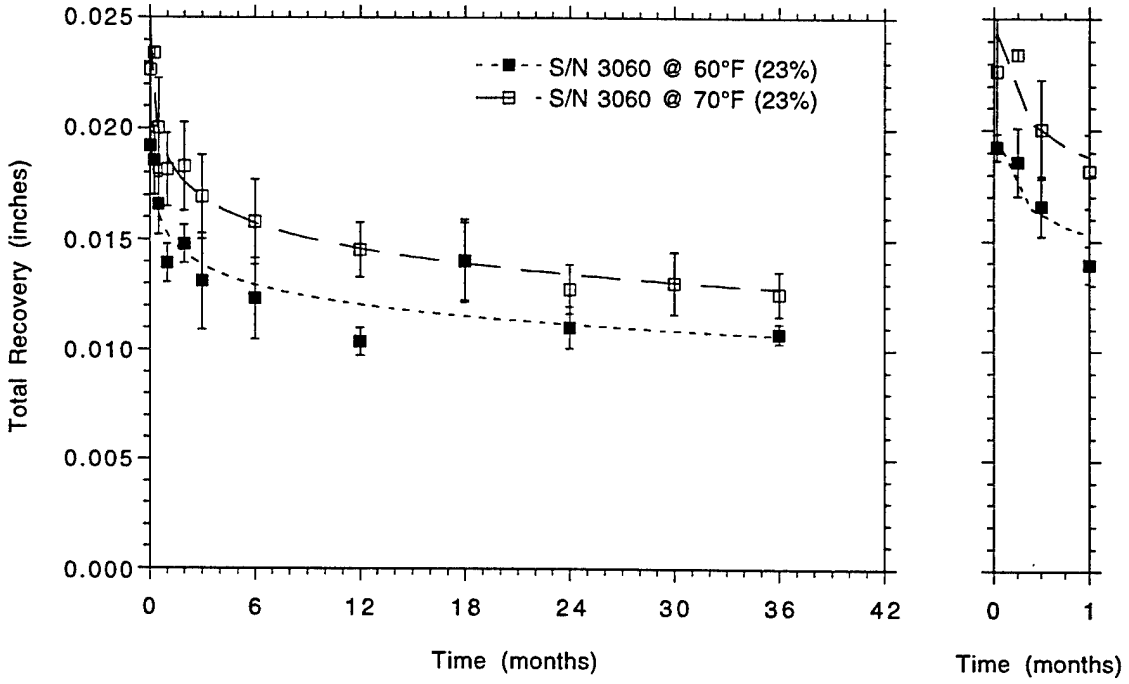

Figure 19. Comparison of total recovery at 2 s vs time under 23% compression for S/N 3060 measured at 60°F and 70°F. (Expanded 1-month recovery period is shown to the right.)

6. Comparison of O-Ring Compression Set Properties

Data are presented here that relate to ASTM D 395-84 method B, which describes the rubber property of compression set under constant deflection in air.[15] As mentioned previously, this method compresses a test specimen to a specific deflection for a specified time and temperature. The test is usually performed on a cylindrical disc specimen, and its residual deformation is measured 30 min after removal from a compressed state. The compression set is expressed as a percentage of the original deflection, where zero percent set constitutes full recovery. Suggested test conditions are 22 and 70 h at 25% compression, under which most reported compression set data are obtained. Although not identical to the conditions described above, compression set data were measured for O-ring specimens S/N 2203 and S/N 3060 after one week under compression at 70°F. The results are shown in Figure 20.

The results in Figure 20 are in agreement with reported compression set data for a Viton B material. The data also show batch-to-batch variation between the two Viton B O-ring samples. In general, the recommended compression (squeeze) for seals is in the range of 15 to 30%. It has been reported that for deflections less than 15%, the compression set results are unreliable. Conversely, at deflections greater than 30% the extra stress can result in premature seal failure.

The compression set variability observed at two different deflections in Figure 20 are further supported by comparing compression set data over all time periods studied for both S/N 2203 and S/N 3060 materials. As can be seen in Figure 21, the data are consistent with what appears to be a rapid reduction in compression set within the first six months followed by a more gradual and predictable change though the remainder of the 36-month period.

During the period of this study, one additional material batch of an unknown (UNK) source was also available for testing. Although sufficient comparative data points are lacking, a limited dataset is presented here for additional insight into batch-to-batch variability. The results are shown in Figure 22 at 17% compression and in Figure 23 at 23% compression.

Comparison of the results in Figures 22 and 23 give a fair indication of the batch-to-batch variability among O-ring samples S/N 2203, S/N 3060, and UNK. Under both deflection conditions a 3 to 19% variability is observed between samples, with compression set properties appearing to be consistently better at the higher initial deflection of 23%.

These measurements have been obtained in the absence of any lubricant. Lubricants are commonly used in dynamic seal applications to avoid dry-contact friction with the gland material and to minimize corrosion. Lubricants can affect the properties of O-ring seals either by shrinkage or swelling. Either result can affect the compression set and resilience properties of the O-ring seals.

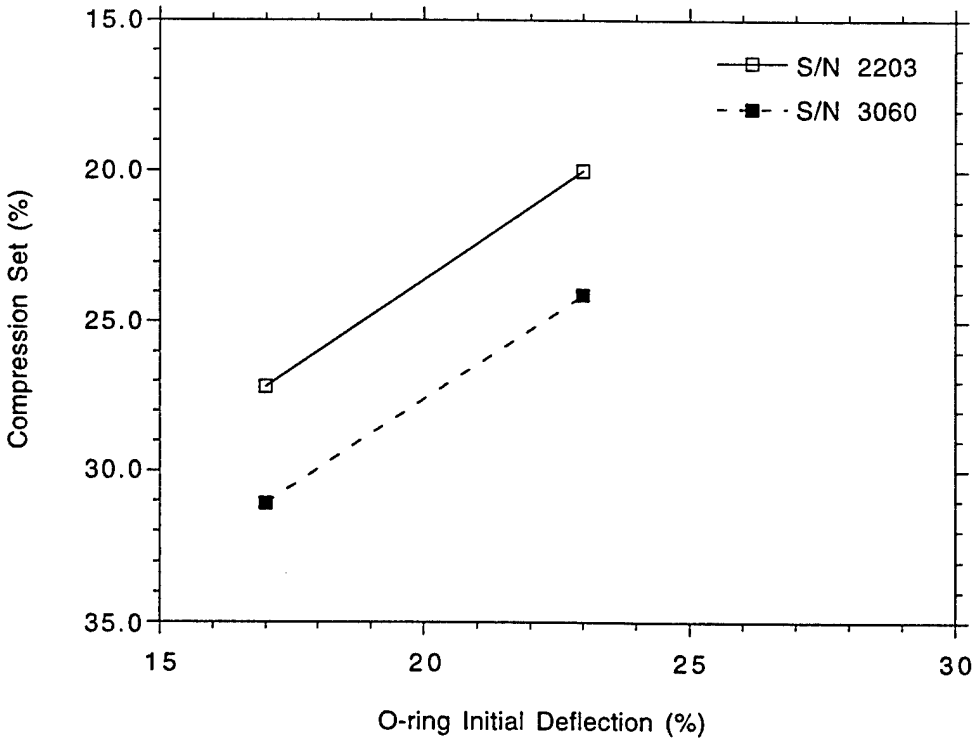

Figure 20. Compression set data for O-ring batches after 1 week at 70°F.

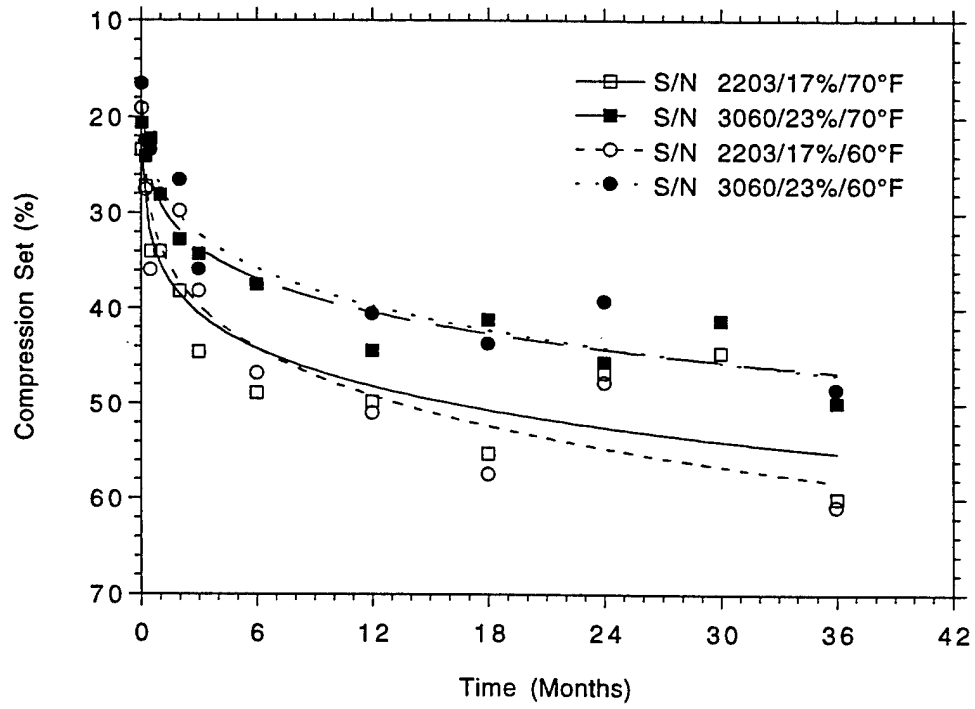

Figure 21. Compression set (Deflection Method) vs time measured 30 min after decompression for all time periods.

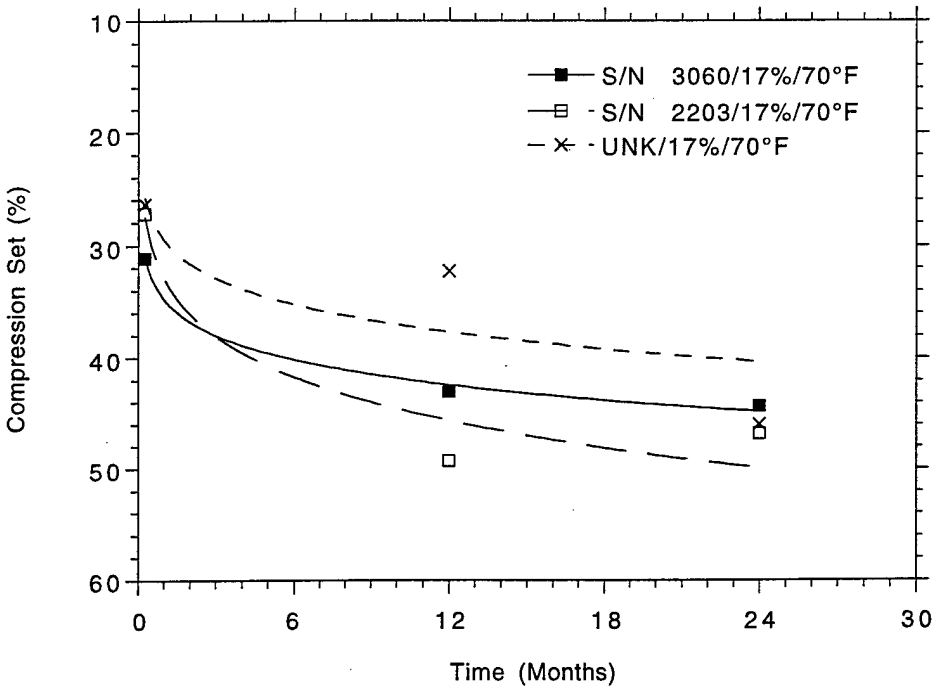

Figure 22. Compression set (Deflection Method) vs time for three different batches of O-ring material at 17% deflection taken 30 min after decompression.

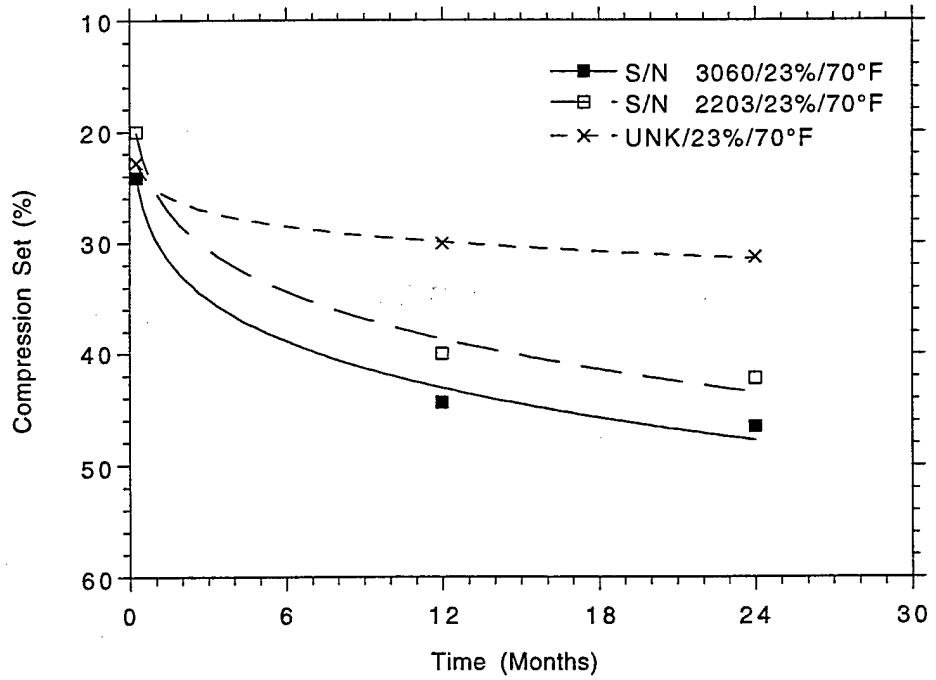

Figure 23. Compression set (Deflection Method) vs time for three different batches of O-ring material at 23% deflection taken 30 min after decompression.

7. Comparison of O-Rings: Greased and Ungreased

During the course of the study of O-rings in the dry or ungreased condition, it was observed that the Viton B O-rings had a tendency to adhere to the aluminum gland at the point of contact. Increasing force was required to remove the O-ring sample from the gland with increasing time under compression. This phenomenon is commonly referred to as dry-contact friction and is attributed to the adhesion characteristics of an elastomer seal material in contact with a dissimilar substrate.[16] In addition to this physical interaction, chemical interactions may also occur between the seal, substrate material, and the surrounding environment, with the potential of leading to corrosion of gland surfaces. Similar concerns were raised when corrosion was found in field joints on destacked motors from Titan 34D-8 and IV-K7.[17] These motors had experienced extended launch pad exposure for periods of up to 540 days. It is primarily for these reasons that most seals are lubricated prior to installation.

Although it was not possible to address all of the potential concerns that were suggested, the study was extended to compare the relative performance of O-rings under both greased and ungreased conditions. Of the material batches available, only S/N 3060 remained, and samples from this batch were used for selected time periods at 70°F under both 17% and 23% compression. One set of samples was assembled under ungreased conditions previously used in this study. Another set was assembled using Dow Corning DC 55 silicone grease similar to that used in loading the space within the O-ring gland not occupied by the O-ring itself. A comparative test matrix using batch S/N 3060 is described in Table 2.

Each O-ring segment was first lubricated with the grease and installed in its respective sample holder. The remaining space in the sample holder cavity was subsequently filled with additional grease. The sample was then confined, as described previously, for the selected time periods. Comparative results for ungreased and greased O-ring samples under 17% compression are shown in Figures 24 and 25, respectively.

Table 2. Compression Test Matrix for Greased and Ungreased S/N 3060 O-Ring Samples at 70°F.

Batch	S/N 3060	S/N 3060	S/N 3060	S/N 3060
Conditions	17%/Ungreased	17%/Greased	23%/Ungreased	23%/Greased
Period				
1 wk	x	x	x	x
1 mo	x	x	x	x
6 mo	x	x	x	x
9 mo	x	x	x	x
12 mo	x	x	x	x

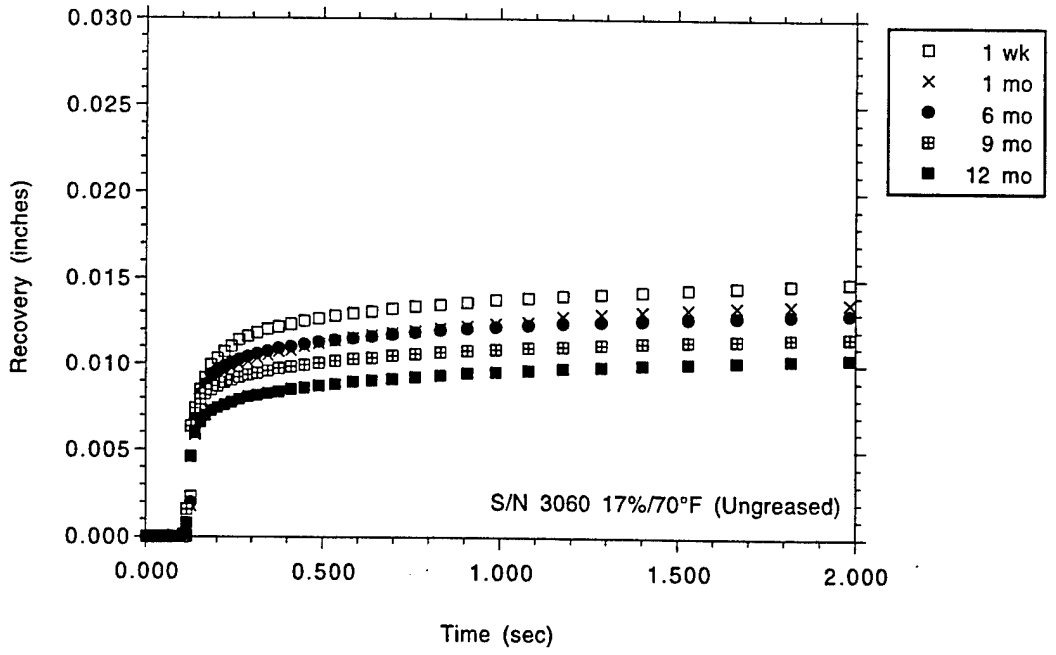

Figure 24. Recovery vs time for O-ring S/N 3060 (ungreased) under 17% compression measured at 70°F.

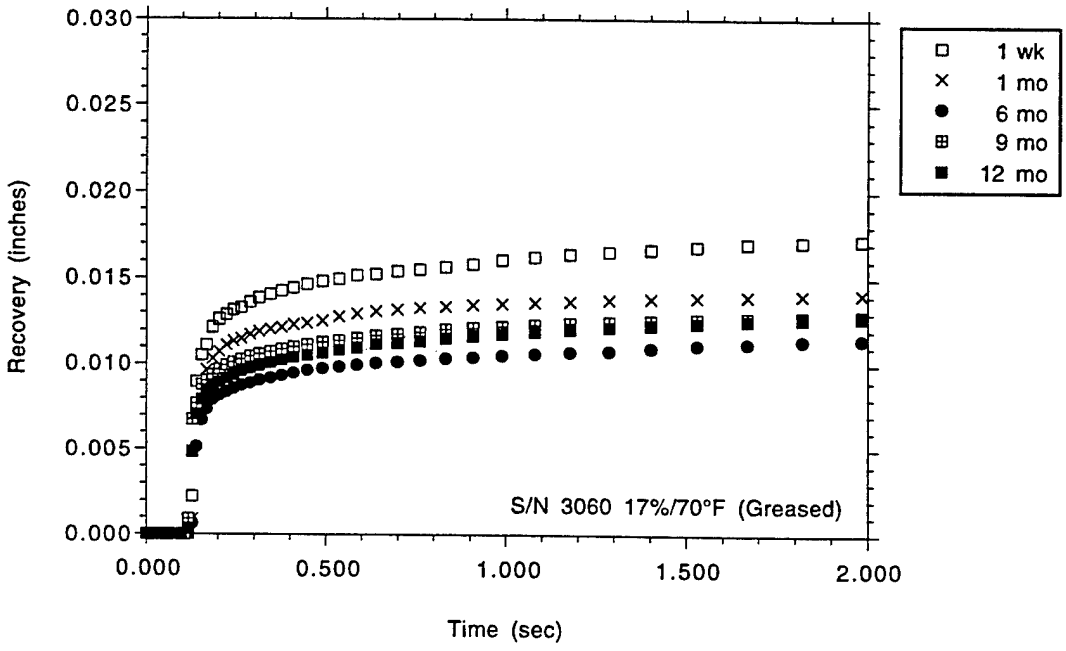

Figure 25. Recovery vs time for O-ring S/N 3060 (greased) under 17% compression measured at 70°F.

The results for S/N 3060 samples under 17% compression indicate a small but distinct trend to higher recovery values for samples that were greased versus those that were ungreased. Again, increasing dry-contact friction was observed for the ungreased samples through all times under compression. Except for the one-week period, some force was required to remove these samples from their sample holder. In contrast, for all time periods under compression, no force was required to remove the greased O-ring samples from the sample holder. A comparable study for S/N 3060 samples under 23% compression showed a similar trend for greased versus ungreased samples. The results for ungreased and greased samples are shown in Figures 26 and 27, respectively. The results observed in the greased/ungreased study indicate, at least through a 12-month period, that dry-contact friction is not a significant factor in O-ring resilience.

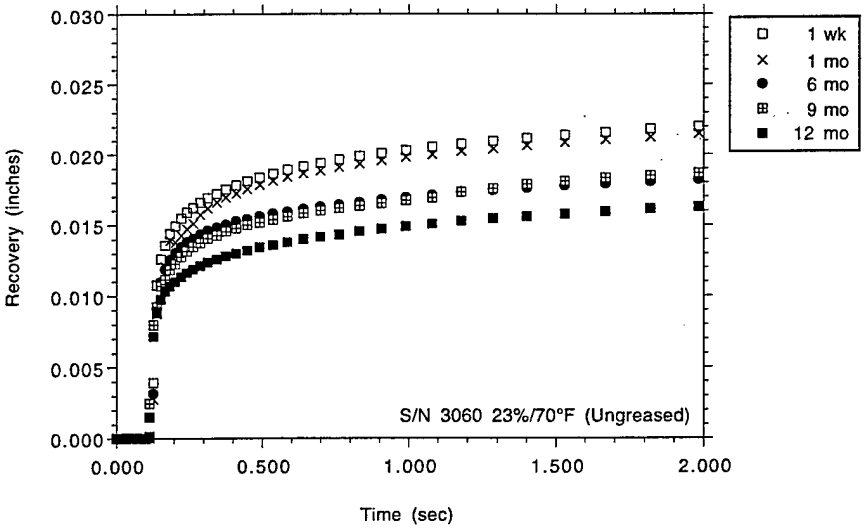

Figure 26. Recovery vs time for O-Ring S/N 3060 (ungreased) under 23% compression measured at 70°F.

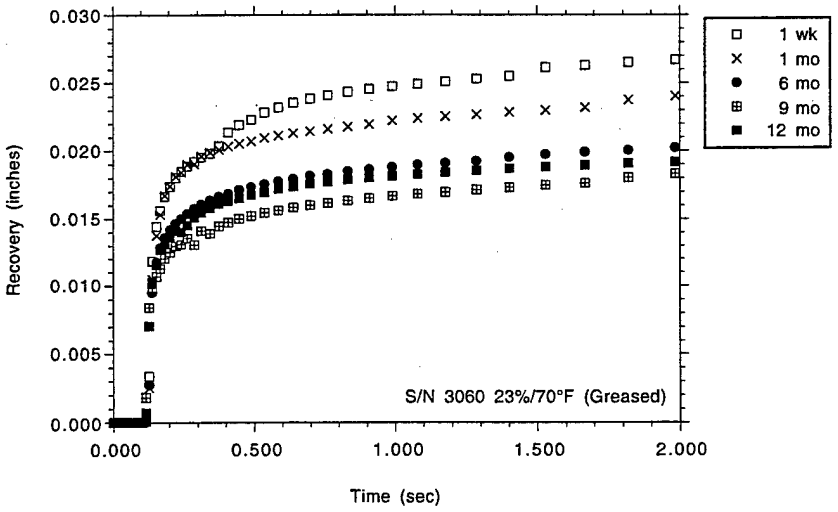

Figure 27. Recovery vs time for O-Ring S/N 3060 (greased) under 23% compression measured at 70°F.

8. Batch-to-Batch Variability of O-Ring Data

Recovery data from different batches under similar conditions were evaluated by comparing data from the greased/ungreased O-ring study with data from the original resilience study. Thus, the results for S/N 2203 shown in Figure 10 are compared with those for S/N 3060 shown in Figure 24. Extracted data at 1 wk, 1 mo, 6 mo, and 12 mo, for these two batches at 17% compression are shown for S/N 2203 in Figure 28 and S/N 3060 in Figure 29. For the shorter time periods (1 wk and 1 mo), batch S/N 2203 appears to have better recovery properties than does batch S/N 3060. Excluding the anomalous behavior described previously for S/N 2203 at the 6-month period, the recovery properties of the two batches would appear to be leveling off in a predictable fashion after much longer periods of time under compression. This behavior has previously been observed for O-ring segments compressed for much longer periods of time, and is consistent with stress relaxation phenomena expected for this material.

Although apparently much less significant at longer time periods under compression, batch-to-batch variability is present and is easily seen in the comparisons made in this report. As such, it is important to assess this data conservatively when considering the extent of recovery from a Viton B material under compression.

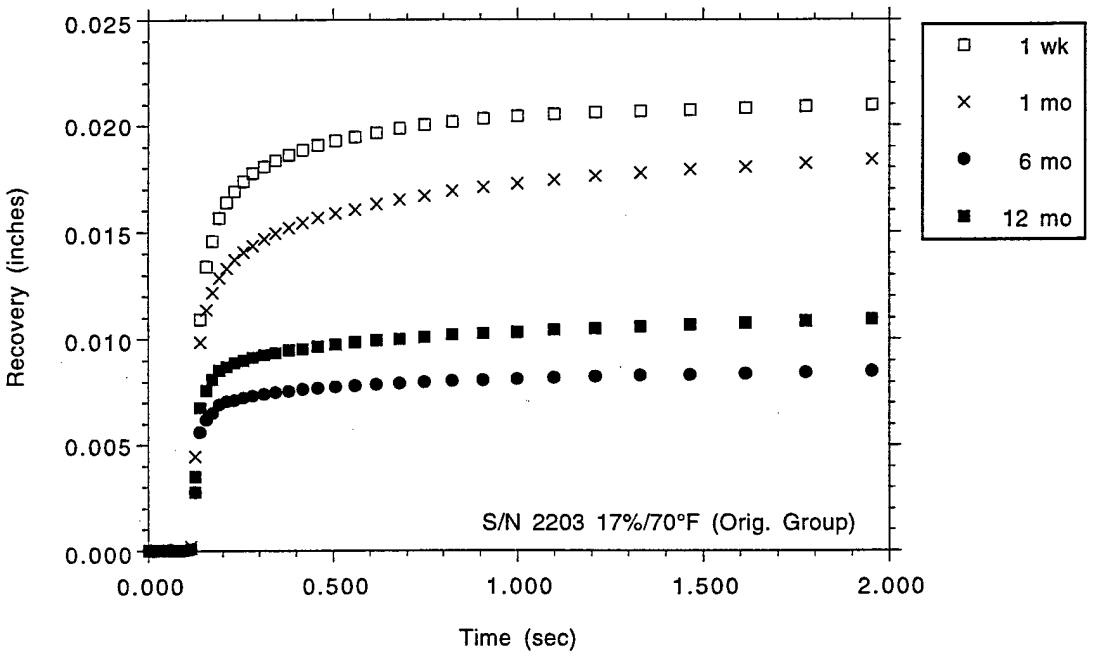

Figure 28. Recovery vs time for O-ring S/N 2203 under 17% compression measured at 70°F.

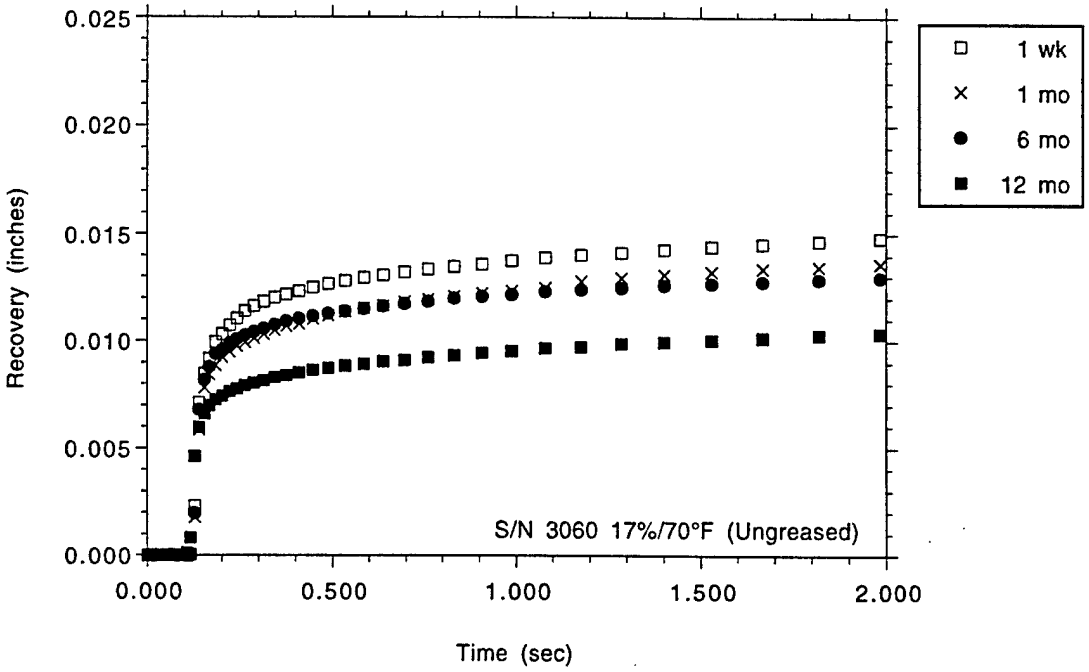

Figure 29. Recovery vs time for O-ring S/N 3060 (ungreased) under 17% compression measured at 70°F.

9. O-Ring Recovery as a Percent of Original Deflection

In order to appreciate the significance of the recovery data heretofore measured in inches, the following section describes the resilience of the Viton B material in terms of percent of the original deflection during the 2-s time interval. The results are first shown for S/N 2203 under 17% compression. Again, in general, the percent recovery at 70°F in Figure 30 is seen to be greater than that at 60°F in Figure 31. These results can be compared with the same data reported in inches as shown in Figures 10 and 11. Similarly, the results for S/N 3060 under 23% compression are shown in terms of percent recovery in Figures 32 and 33. These results can also be compared to the data reported in inches in Figures 15 and 16.

The percent recovery at 2 s for all time periods under compression are then compared at the two temperatures for each O-ring material. The results are shown for S/N 2203 in Figure 34 and for S/N 3060 in Figure 35. They can be compared with the same data reported in inches in Figures 18 and 19, respectively. At both 17% and 23% compression, the data indicate a lower percent recovery at the lower temperature (60°F) and that, under all conditions, recovery seems to taper off and become less sensitive somewhere beyond the 3-month period.

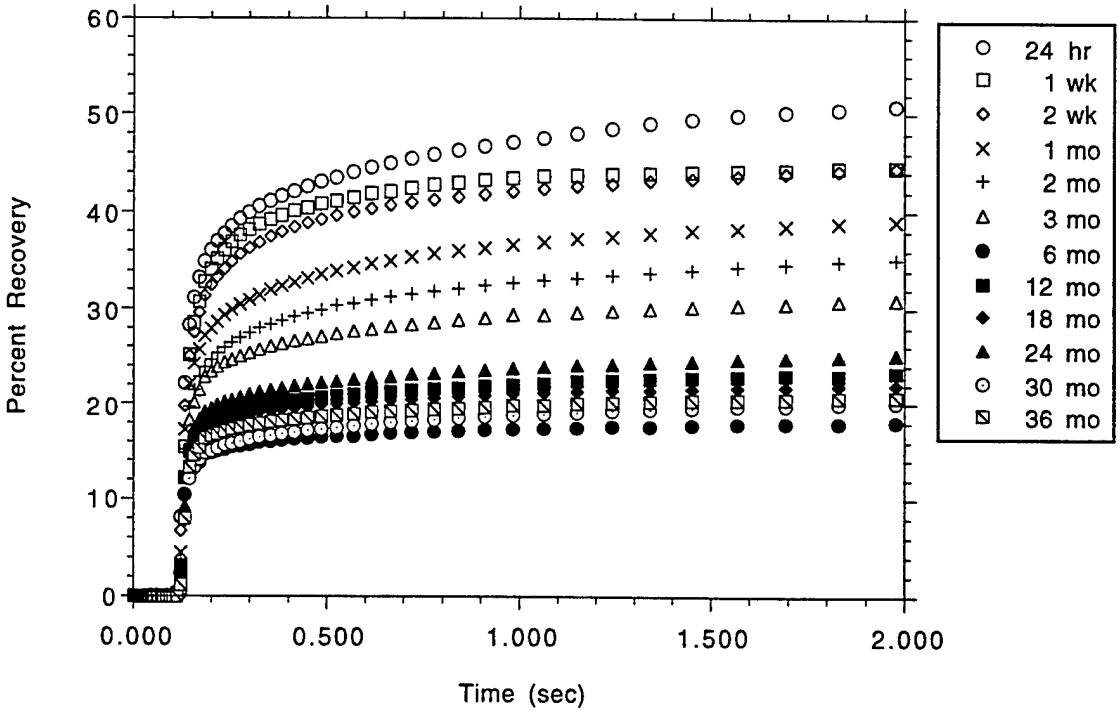

Figure 30. Percent recovery from 17% deflection for O-ring S/N 2203 measured at 70°F.

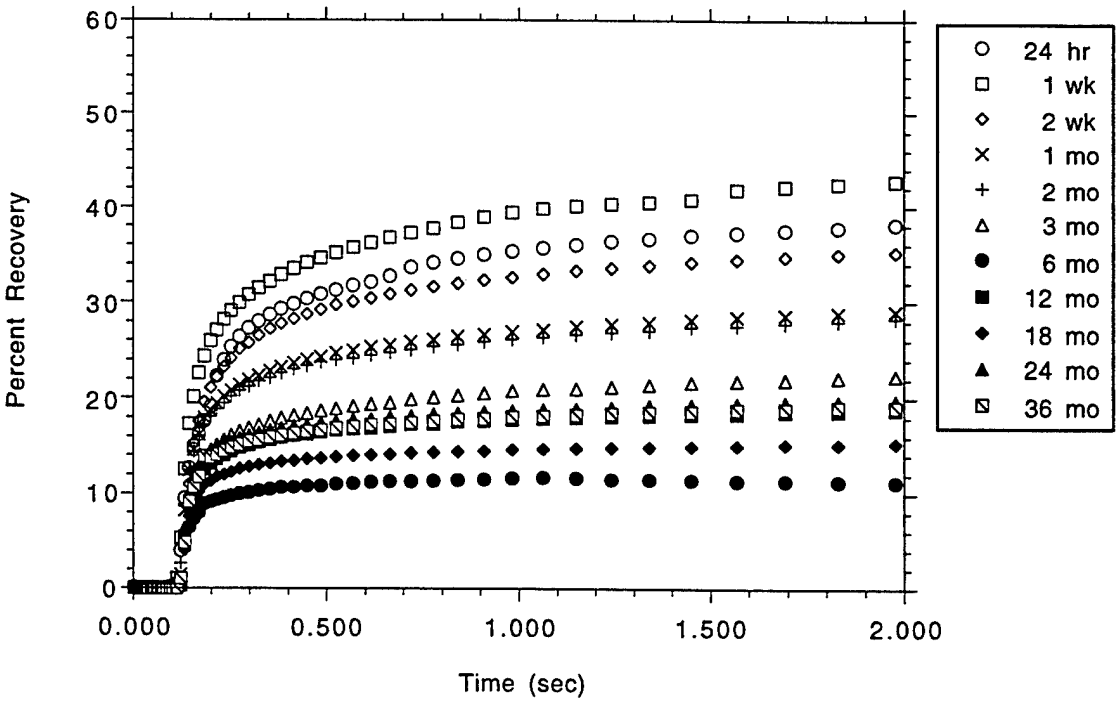

Figure 31. Percent recovery from 17% deflection for O-ring S/N 2203 measured at 60°F.

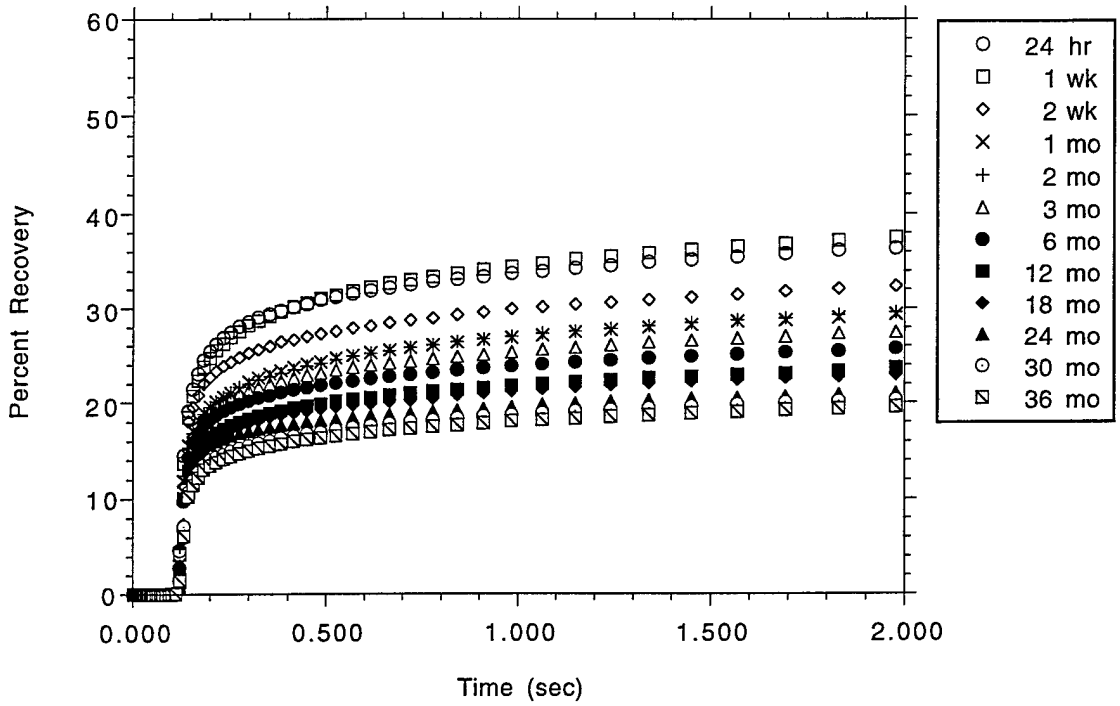

Figure 32. Percent recovery from 23% deflection for O-ring S/N 3060 measured at 70°F.

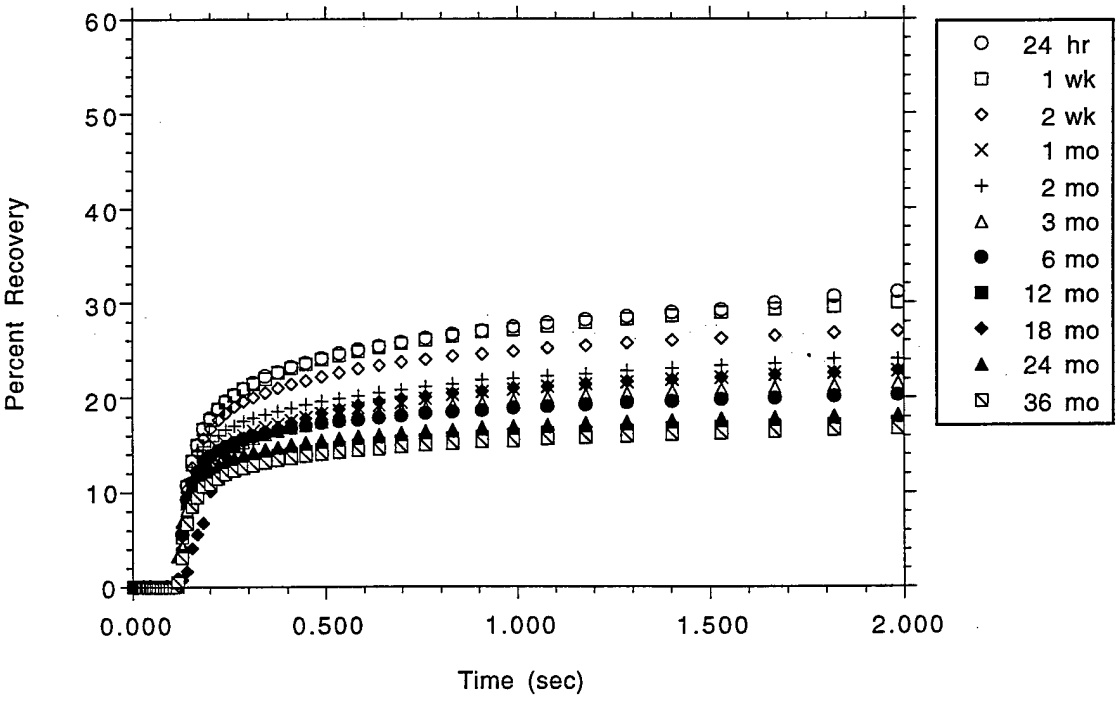

Figure 33. Percent recovery from 23% deflection for O-ring S/N 3060 measured at 60°F.

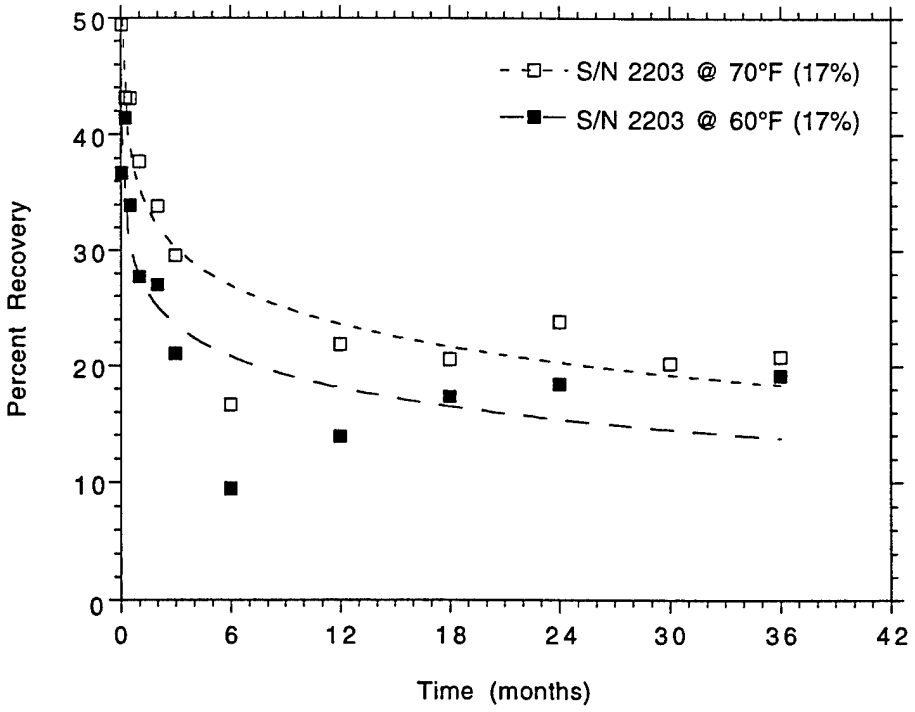

Figure 34. Comparison of percent recovery at 2 s from 17% deflection for O-ring S/N 2203 measured at 60°F and 70°F.

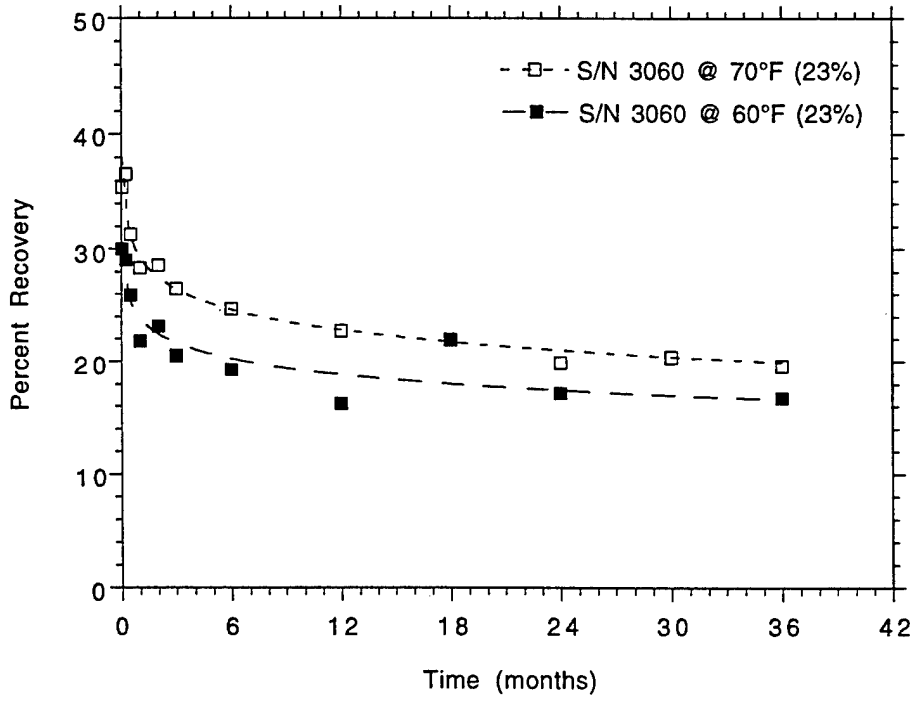

Figure 35. Comparison of percent recovery at 2 s from 23% deflection for O-ring S/N 3060 measured at 60°F and 70°F.

10. Resilience and Gap Opening Rate

The predicted pressurized and unpressurized gap opening rates for the Titan IV SRM are shown in Figure 3. Half-scale O-ring sealing tests were developed in order to simulate Titan SRM O-ring/field joint characteristics.[18] A computer simulation program was developed for the purpose of understanding O-ring sealing behavior based on the sealing test results.[19] The half-scale testing procedure incorporated a pre-selected hydrostatic pressure to reach the maximum O-ring gap opening. After specified delay times, pre-determined gas pressure is released and charges onto the O-ring cavity. The results were classified into three groups: no leak; leak with reseal; leak without reseal. The half-scale O-ring tests did confirm two important facts. First, the side pressure-assisted recovery is an integral part of the O-ring sealing properties. Second, as long as the maximum gap opening is not excessive and the initial O-ring squeeze is above a minimum allowable, the worst that can happen is "leak with reseal." The simulation computer program also predicts that instantaneous charging of the O-ring can almost guarantee no leak at temperatures as low as 30°F.

Instantaneous charging is common to standard O-ring designs where the application of pressure to the seal is simultaneous with the movement of the joint under the same pressure. This allows the O-ring to move into the corner of the groove where the sealing is achieved before the two sealing surfaces are displaced with respect to each other. In the SRM, where joint roll may precede side-pressure assist, the seal depends on O-ring resilience to close the gap. If the O-ring is unable to follow the decompression gap opening, any leaking gases at the joint are likely to leak past the O-ring. At high rates of pressurization, the O-ring might reseal if thermal damage to the O-ring from hot propellant gases is not too severe.

Another experimental study was performed to evaluate the ability of a Viton B O-ring to seal when the displacement of the sealing surfaces preceded the application of side pressure to the O-ring gland.[20] The results from that study showed that for the Titan SRM design configuration, when pressurization is delayed more than 500 ms, the permissible joint deflection is determined by the viscoelastic properties of the O-ring at a given temperature. If, however, the pressure is applied to the O-ring as the joint deforms, proper sealing is achieved down to 35°F with a pressurization rate of 5000 psi/s. With delayed pressurization, the service temperature may be limited to greater than 50°F for joints with nominal dimensions.

The collected data for resilience of Viton B O-rings under compression for durations of up to 36 months are compared to the predicted pressurized and unpressurized gap opening rates previously shown in Figure 3. Resilience for O-ring samples S/N 3060 under 23% compression at 60°F and 70°F are shown overlayed with the predicted O-ring gap openings in Figures 36 and 37. Those for samples S/N 2203 under 17% compression at 60°F and 70°F are shown in Figures 38 and 39.

In Figures 36–39, the lower dashed curve represents the predicted gap opening with time for the Titan SRM field joint with the butt joint compression face sealed. The upper curve represents a butt joint

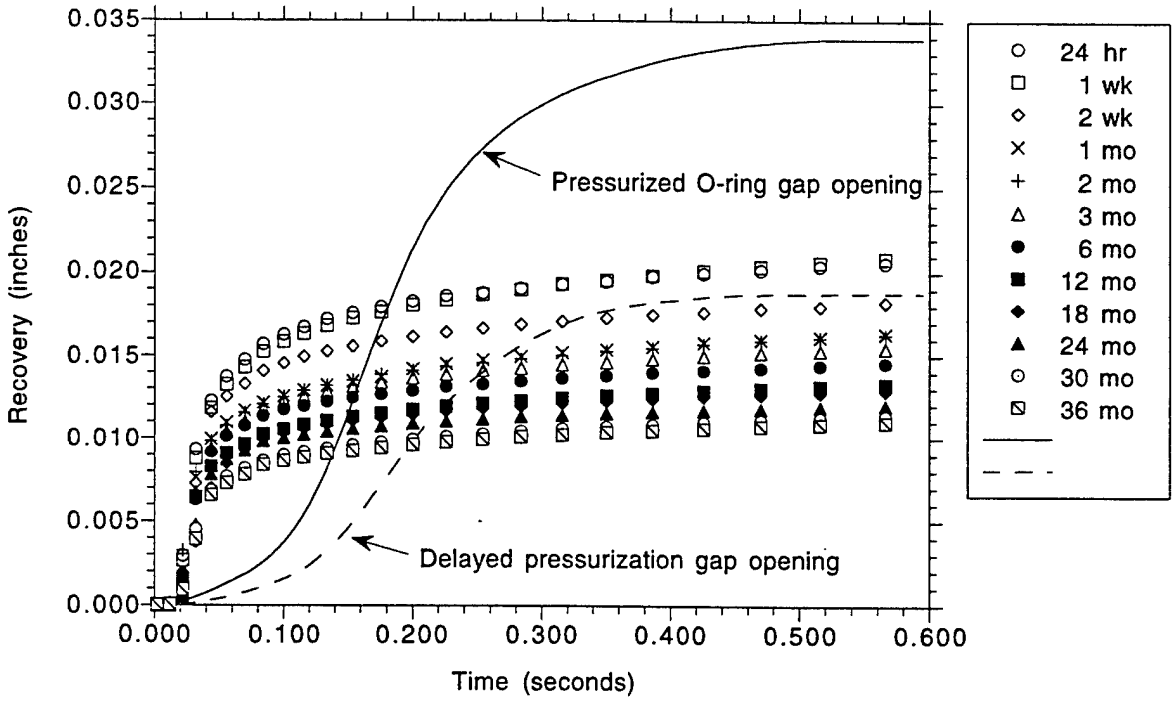

Figure 36. Comparison of recovery of S/N 3060 at 23%/70°F and SRM predicted gap opening rate.

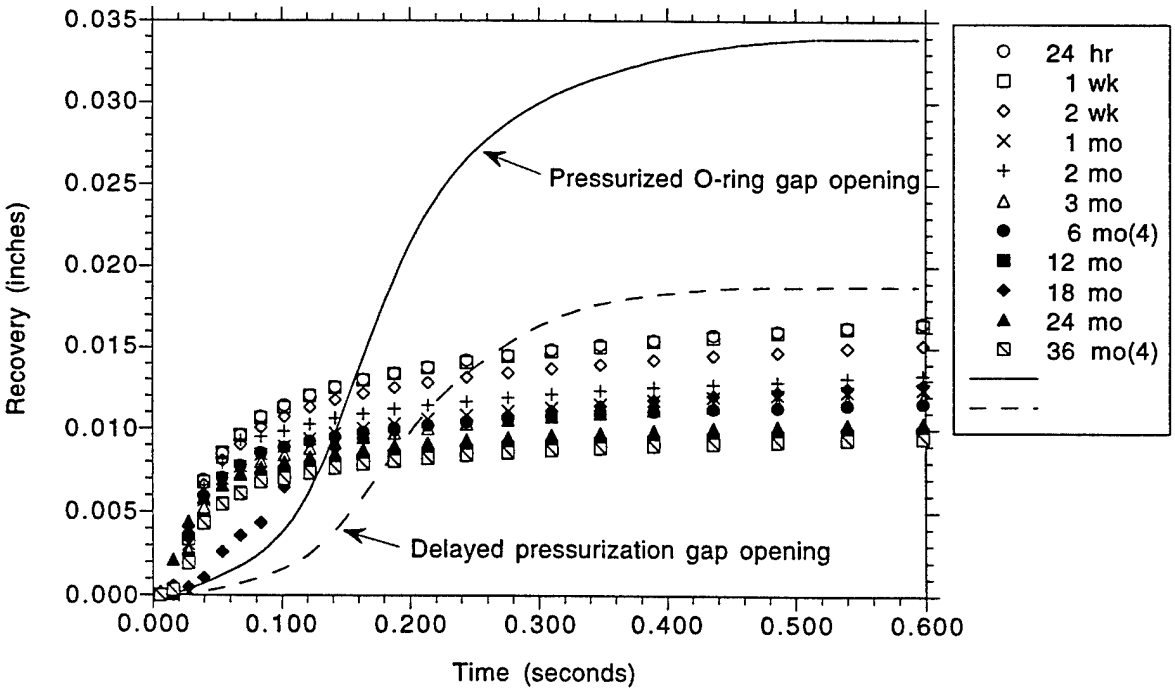

Figure 37. Comparison of recovery of S/N 3060 at 23%/60°F and SRM predicted gap opening rate.

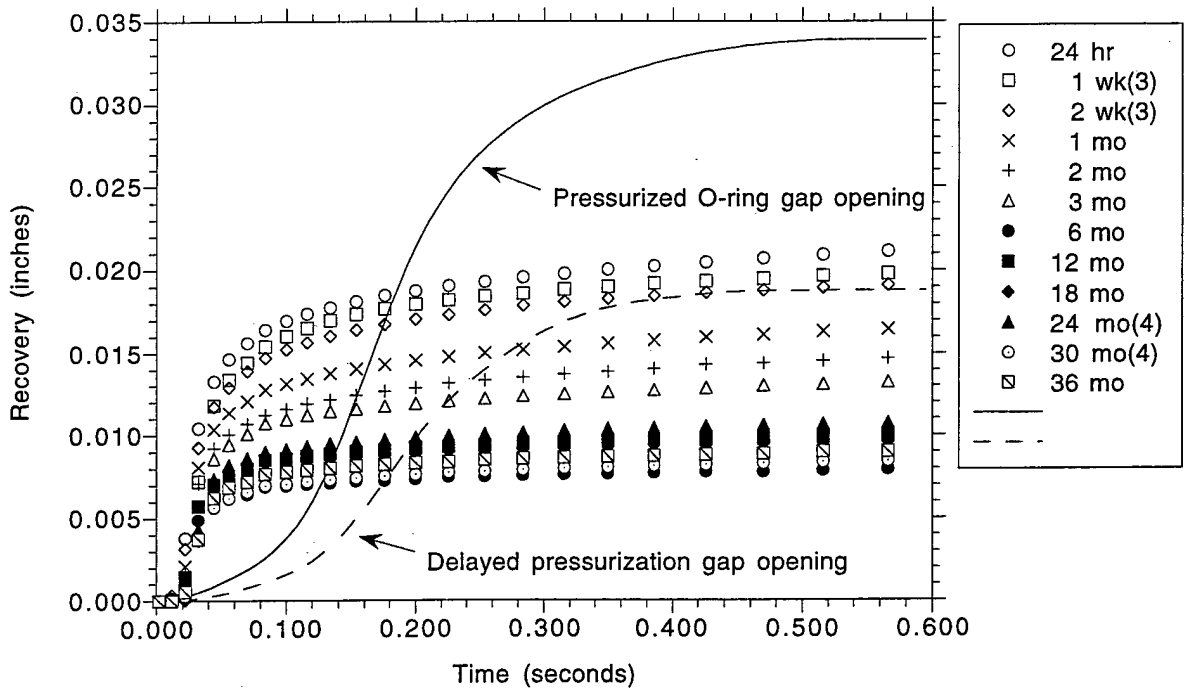

Figure 38. Comparison of recovery of S/N 2203 at 17%/70°F and SRM predicted gap opening rate.

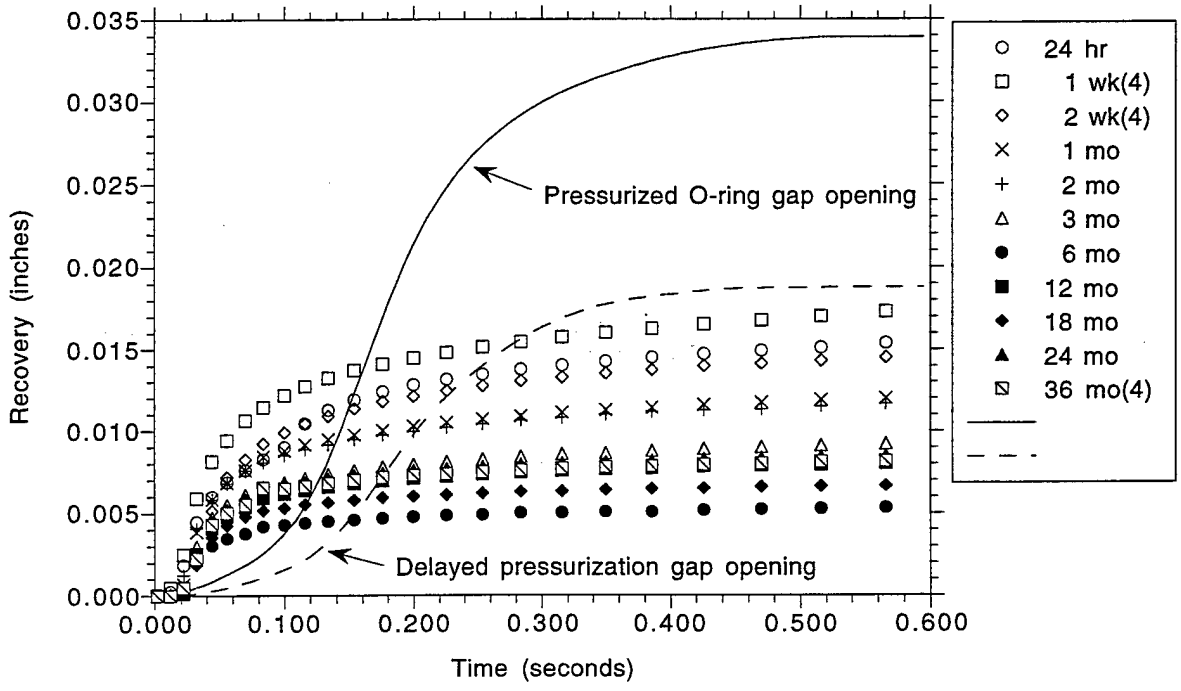

Figure 39. Comparison of recovery of S/N 2203 at 17%/60°F and SRM predicted gap opening rate.

open case, allowing simultaneous charging of the O-ring. The contrasting data points represent O-ring recovery curves up to 36 months under compression. In every case, the slope of the resilience curve exceeds that of the gap displacement curves in the initial stages of ignition. The rate of recovery of the O-ring is seen to be quite rapid in the first few milliseconds from ignition. As expected, with increasing time under compression, the initial rate of recovery is reduced with a consequent reduced ability to track the gap opening. Where the slope of the resilience curve is greater than the slope of the gap displacement curve, this would be considered a no-leak condition. Without side-pressure assist, the O-ring would start leaking when the slope of the resilience curve is less than that of the slope of gap opening. Any delayed pressurization would result in a shift from the unpressurized displacement curve to the pressurized displacement curve.

In the absence of side-pressure assist, the results indicate that only for the shortest times under compression and particularly at the higher temperature studied (70°F) do the Viton B O-ring recovery properties provide a no-leak condition through MEOP. This appears to be consistent with results for resilience of Viton B materials described in other reports.[21,22] By sliding the resilience curves along the time axis until the slopes of the curves are less than the slope of the unpressurized gap opening curve, the time to O-ring leakage can be calculated for each compression duration.

The pad life requirement for O-ring seals was specified as 12 months. The longest period for which a Titan SRM had been stacked prior to a successful launch was approximately 14 months. Assuming no leakage or leakage with reseal has occurred, it appears that side-pressure-assisted recovery is essential to O-ring sealing capability. From the data in Figures 36–39, a minimum criteria for resilience for O-rings in the Titan SRM configuration for the temperature range studied can be established.

11. Summary

The results of the data for Viton B O-ring material under compression for up to 36 months show an initial rapid rate of recovery in the first 100 ms, diminishing significantly during the next 300 ms, and essentially leveling off through the end of the 2-s test period. The effect of temperature on recovery properties under compression is quite significant for a fluorocarbon elastomer such as Viton B. In general, for both batches tested, there is a dramatic reduction in the ability for the O-ring material to recover when the temperature is lowered from 70°F to 60°F. This is intrinsic to Viton B, which undergoes a rapid increase in hardness with decreasing temperature near ambient. It is this intrinsic behavior of Viton B that is the driving force behind a future replacement material that retains desirable properties at high temperatures but is much less sensitive to temperatures below ambient.

With the exception of some anomalous behavior at certain time periods, the trend of the data is toward reduced recovery with both increasing time and decreasing temperature under compression. The extent of recovery follows the expected pattern for a material with low compression set properties. Previous reports on Viton resilience are in reasonable agreement with the data reported herein for the shorter time periods.

Although samples were limited, batch-to-batch variability among O-ring samples appeared to be most prominent at shorter periods under compression. At longer periods, the compression set characteristics result in more predictable resilience properties with much less variability.

The recovery characteristics among batches at the two compression squeeze values of 17% and 23% were similar in that they were a comparable fraction of the initial deflection. This is in keeping with the compression set characteristics of the elastomer.

O-rings are usually lubricated and installed in an O-ring gland that is filled with additional grease. The application of grease can provide a number of positive features to the assembly. These include facile O-ring mobility under dynamic compression, reduced chemical interaction between O-ring and gland materials, and partial swelling of the O-ring material that serves to enhance resilience. Comparison of an O-ring material under both greased and ungreased conditions did show some improvement when in the greased condition versus the ungreased condition.

The differences in the O-ring test environment described in this report compared to that of the launch vehicle environment are expected to have minimal impact on resilience. The data presented here, supported by comparable compression set and resilience characteristics for O-rings published elsewhere, are expected to closely represent resilience values that would be exhibited during launch.

12. Conclusion

The results showed that the resilience of Viton B O-rings was very sensitive to temperature and that resilience is reduced dramatically as the temperature is lowered from 70°F to 60°F. Also, with increasing time under compression, which is of concern where delayed launches result in segments being stacked for unpredictably long periods, resilience is also significantly reduced. The greatest rate of change in O-ring resilience occurred within the first three months under compression. After three months, the rate of change in O-ring resilience continued at a much lower rate throughout the 36-month test period. The results also indicate that, in the absence of side-pressure assist, a no-leak condition exists only for the shortest times under compression, and particularly at the higher temperature condition. Since successful Titan launches have occurred with pad life as long as 14 months, it appears that side-pressure-assisted recovery is essential to O-ring sealing ability. The data on the resilience characteristics of Viton B O-rings under long-term compression was obtained in real time rather than extrapolated from elevated temperature data. These data can be used in conjunction with structural analysis of joint motion to predict O-ring seal performance during extended periods. Variability in properties among Viton B O-ring batches also appeared to be a factor that should be taken into consideration when evaluating sealing ability under specific operating conditions.

References

1. W. P. Rogers (Chairman), "The Report of the Presidential Commission on the Space Shuttle Challenger Accident," U. S. Government Printing Office, Washington, D. C., 1986.

2. A. J. McDonald, "Redesigned Solid Rocket Motor Enhancements," Morton Thiokol, Inc., Brigham City, UT. AIAA-89-2620, AIAA/ASME/SAE/ASEE 25th Joint Propulsion Conference, Monterey, CA, July 10–12, 1989.

3. N. Perry, N. Eddy, L. Gruet, and J. Maw, "Design and Thermal Verification of the Space Shuttle Redesigned Solid Rocket Motor Field Joint," Thiokol Corporation, Brigham City, UT. AIAA-89-2775, AIAA/ASME/SAE/ASEE 25th Joint Propulsion Conference, Monterey, CA, July 10-12, 1989.

4. A. J. McDonald, "Return to Flight with the Redesigned Solid Rocket Motor," Morton Thiokol, Inc., Brigham City, UT. AIAA-89-2404, AIAA/ASME/SAE/ASEE 25th Joint Propulsion Conference, Monterey, CA, July 10-12, 1989.

5. C. L. Lach, "Effect of Temperature and O-Ring Gland Finish on Sealing Ability of Viton V747-75," NASA TP-3391, NASA Langley Research Center, Hampton, VA, November 1993.

6. R. G. Arnold, A. L. Barney, and D. C. Thompson, "Fluoroelastomers," *Rubber Chemistry and Technology*, Vol. 46 #3, pp. 619–52, 1973.

7. W. M. Grootaert, G. H. Millet, and A. T. Worm, "Elastomers, Synthetic (Fluorinated) ," *Encyclopedia of Chemical Technology*, 4th Edition, Vol. 8, John Wiley & Sons, 1993, pp. 990–1005.

8. M. M. Lynn and A. T. Worm, "Fluorocarbon Elastomers," *Encyclopedia of Polymer Science and Engineering*, 2nd Edition, Vol. 7, John Wiley & Sons, 1987, pp. 257–269.

9. A. Kemp et al., "Qualification Test Plan for Viton GLT O-Ring Half-Scale Dynamic Testing," United Technologies Chemical Systems Division, CSD 4622-94-032, September 23, 1994.

10. R. K. Flitney, B. S. Nau, and D. Reddy, *The Seal Users Handbook*, 3rd Edition, 1984, p.36.

11. S. L. Zacharius, "Resilience Data for a Viton O-ring," ATM-87(2443-09)-30, 23 February 1987; "Viton O-Ring Recovery Data, Update," ATM-93(3530-03)-36, 9 July 1993; The Aerospace Corporation, Los Angeles, CA.

12. *Parker O-Ring Handbook* ORD 5700, pp. A3-10, Parker Hannifin Corporation.

13. R. G. Stacer, D. M. Husband, and H. L. Stacer, "Viscoelastic Response and Adhesion Properties of Highly Filled Elastomers," *Rubber Chemistry and Technology*, Vol. 60 (2), pp. 227–244, 1987.

14. G. A. Miller and L. H. Sperling, *Polymer Engineering and Science*, Vol. 22, No. 8, pp. 478–483, 1982.

15. ASTM D 395-89 (Reapproved 1994): Standard Test Methods for Rubber Property—Compression Set. Annual Book of ASTM Standards, Section 9, Volume 09.01, 1997.

16. *Variseal Design Guide*, American Variseal Corporation, Broomfield, CO, pp. 9-14.

17. S. W. Frost and F. D. Ross, "Corrosion of the SRM Joint O-Ring Seal Area and SRM Pad-Life Extension," ATM-94(4530-03)-16, 28 March 1994; The Aerospace Corporation, Los Angeles, CA.

18. E. R. Mills, "Test Report for the Viton O-ring Material", CSD Report, TR-4165-004-NC, Titran 34D Recovery Program, 30 March 1987.

19. C. C. Lee, "Review of Half-Scale O-Ring Sealing Test", ATM NO.: 88(3447-04)-7, 16 February 1988; The Aerospace Corporation, Los Angeles, CA.

20. D. A. Durran, "Pressure Tests on Titan O-Ring", ATM NO.: 86(6443-09)-14, 18 June 1986; The Aerospace Corporation, Los Angeles, CA.

21. L. M. Fraser, J. W. Martin, and H. E. McCormick, "A New Test for Seals: High Temperature Resilience," *Elastomerics*, Vol. 116 (4), pp. 44-9, 1984.

22. C. L. Lach, "Effect of Temperature and Gap Opening Rate on the Resiliency of Candidate Solid Rocket Boostser O-Ring Materials," NASA TP-3226, NASA Langley Research Center, Hampton, VA, June 1992.

LABORATORY OPERATIONS

The Aerospace Corporation functions as an "architect-engineer" for national security programs, specializing in advanced military space systems. The Corporation's Laboratory Operations supports the effective and timely development and operation of national security systems through scientific research and the application of advanced technology. Vital to the success of the Corporation is the technical staff's wide-ranging expertise and its ability to stay abreast of new technological developments and program support issues associated with rapidly evolving space systems. Contributing capabilities are provided by these individual organizations:

Electronics and Photonics Laboratory: Microelectronics, VLSI reliability, failure analysis, solid-state device physics, compound semiconductors, radiation effects, infrared and CCD detector devices, data storage and display technologies; lasers and electro-optics, solid state laser design, micro-optics, optical communications, and fiber optic sensors; atomic frequency standards, applied laser spectroscopy, laser chemistry, atmospheric propagation and beam control, LIDAR/LADAR remote sensing; solar cell and array testing and evaluation, battery electrochemistry, battery testing and evaluation.

Space Materials Laboratory: Evaluation and characterizations of new materials and processing techniques: metals, alloys, ceramics, polymers, thin films, and composites; development of advanced deposition processes; nondestructive evaluation, component failure analysis and reliability; structural mechanics, fracture mechanics, and stress corrosion; analysis and evaluation of materials at cryogenic and elevated temperatures; launch vehicle fluid mechanics, heat transfer and flight dynamics; aerothermodynamics; chemical and electric propulsion; environmental chemistry; combustion processes; space environment effects on materials, hardening and vulnerability assessment; contamination, thermal and structural control; lubrication and surface phenomena.

Space Science Applications Laboratory: Magnetospheric, auroral and cosmic ray physics, wave-particle interactions, magnetospheric plasma waves; atmospheric and ionospheric physics, density and composition of the upper atmosphere, remote sensing using atmospheric radiation; solar physics, infrared astronomy, infrared signature analysis; infrared surveillance, imaging, remote sensing, and hyperspectral imaging; effects of solar activity, magnetic storms and nuclear explosions on the Earth's atmosphere, ionosphere and magnetosphere; effects of electromagnetic and particulate radiations on space systems; space instrumentation, design fabrication and test; environmental chemistry, trace detection; atmospheric chemical reactions, atmospheric optics, light scattering, state-specific chemical reactions and radiative signatures of missile plumes.

Center for Microtechnology: Microelectromechanical systems (MEMS) for space applications; assessment of microtechnology space applications; laser micromachining; laser-surface physical and chemical interactions; micropropulsion; micro- and nanosatellite mission analysis; intelligent microinstruments for monitoring space and launch system environments.

Office of Spectral Applications: Multispectral and hyperspectral sensor development; data analysis and algorithm development; applications of multispectral and hyperspectral imagery to defense, civil space, commercial, and environmental missions.